

AD _____

Award Number: W81XWH-04-1-0500

TITLE: Structure Optimization of 21,23-Core-Modified Porphyrins Absorbing Long-Wavelength Light as Potential Photosensitizers Against Breast Cancer Cells

PRINCIPAL INVESTIGATOR: Michael R. Detty, Ph.D.

CONTRACTING ORGANIZATION: New York State University
Amherst, NY 14228-2567

REPORT DATE: April 2008

TYPE OF REPORT: Final

PREPARED FOR: U.S. Army Medical Research and Materiel Command
Fort Detrick, Maryland 21702-5012

DISTRIBUTION STATEMENT: Approved for Public Release;
Distribution Unlimited

The views, opinions and/or findings contained in this report are those of the author(s) and should not be construed as an official Department of the Army position, policy or decision unless so designated by other documentation.

REPORT DOCUMENTATION PAGE				Form Approved OMB No. 0704-0188	
Public reporting burden for this collection of information is estimated to average 1 hour per response, including the time for reviewing instructions, searching existing data sources, gathering and maintaining the data needed, and completing and reviewing this collection of information. Send comments regarding this burden estimate or any other aspect of this collection of information, including suggestions for reducing this burden to Department of Defense, Washington Headquarters Services, Directorate for Information Operations and Reports (0704-0188), 1215 Jefferson Davis Highway, Suite 1204, Arlington, VA 22202-4302. Respondents should be aware that notwithstanding any other provision of law, no person shall be subject to any penalty for failing to comply with a collection of information if it does not display a currently valid OMB control number. PLEASE DO NOT RETURN YOUR FORM TO THE ABOVE ADDRESS.					
1. REPORT DATE 01-04-2008		2. REPORT TYPE Final		3. DATES COVERED 1 Apr 2003 – 31 Mar 2008	
4. TITLE AND SUBTITLE Structure Optimization of 21,23-Core-Modified Porphyrins Absorbing Long-Wavelength Light as Potential Photosensitizers Against Breast Cancer Cells				5a. CONTRACT NUMBER	
				5b. GRANT NUMBER W81XWH-04-1-0500	
				5c. PROGRAM ELEMENT NUMBER	
6. AUTHOR(S) Michael R. Detty, Ph.D. Email: mdetty@buffalo.edu				5d. PROJECT NUMBER	
				5e. TASK NUMBER	
				5f. WORK UNIT NUMBER	
7. PERFORMING ORGANIZATION NAME(S) AND ADDRESS(ES) New York State University Amherst, NY 14228-2567				8. PERFORMING ORGANIZATION REPORT NUMBER	
9. SPONSORING / MONITORING AGENCY NAME(S) AND ADDRESS(ES) U.S. Army Medical Research and Materiel Command Fort Detrick, Maryland 21702-5012				10. SPONSOR/MONITOR'S ACRONYM(S)	
				11. SPONSOR/MONITOR'S REPORT NUMBER(S)	
12. DISTRIBUTION / AVAILABILITY STATEMENT Approved for Public Release; Distribution Unlimited					
13. SUPPLEMENTARY NOTES Original contains colored plates: ALL DTIC reproductions will be in black and white.					
14. ABSTRACT In the first year, we made eighteen new 21,23-core modified porphyrins, determined their photophysical properties, and evaluated the biological properties of them. In the second year, the research focused on 1) analyzing quantitative structure-activity relationships (QSAR) of the porphyrins prepared in the first year, 2) establishing new synthetic methods for novel structures and preparing them. In the third year, the structures of two derivatives were determined unambiguously by x-ray crystallography. A series of carboxylic acid-substituted dithiaporphyrins was prepared with different length aliphatic spacers between porphyrin and acid. The efficiency of them was studied and mode of binding with lipid model was studied. In addition, we made novel structures having different core and meso substitution patterns and tested them with in vitro model.					
15. SUBJECT TERMS Photodynamic therapy, breast cancer, core-modified porphyrin, in vitro biological activity					
16. SECURITY CLASSIFICATION OF:			17. LIMITATION OF ABSTRACT	18. NUMBER OF PAGES	19a. NAME OF RESPONSIBLE PERSON
a. REPORT U	b. ABSTRACT U	c. THIS PAGE U			USAMRMC
			UU	32	19b. TELEPHONE NUMBER (include area code)

Introduction

The objectives of this project are two folds: one is to train the former PI, Dr. Youngjae You, as an photodynamic cancer therapy expert in breast cancer research and the other is to perform the research to optimize the structure of 21,23-core-modified porphyrins as potential photosensitizers that are able to absorb long-wavelength light for treating breast cancer.

Photodynamic therapy (PDT) is a promising new treatment for cancer that is expected to be more selective and less toxic compared to current major treatment regimes such as surgery, chemotherapy and radiotherapy.¹ However, there are only a few photosensitizers approved for PDT, and they have properties far from an ideal photosensitizer.² The overall goal of this project is to obtain novel photosensitizers from 21,23-core-modified porphyrins targeting mitochondrial peripheral benzodiazepine receptor (PBR) for the PDT treatment of breast cancers.

21,23-Core-modified porphyrins are an attractive chemical entity as a lead compound with several merits: they absorb longer wavelengths of light ($\geq 695\text{nm}$) and have established synthetic procedures that permit diverse structural modification.³⁻⁵ PBR has been aimed as a primary target of various photosensitizers.⁶⁻⁸ More interestingly, previous studies have shown that most breast cancer cell lines produce the PBR and, in several more aggressive breast cancer cell lines, the PBR is over-expressed.⁹⁻¹¹ Thus, we hypothesized that the design of core-modified porphyrins structurally similar to protoporphyrin IX, which has been known as natural ligand of PBR, might lead to more efficient photosensitizers for the treatment of breast cancers.

Body

First year

In the course of accomplishing the first-year goals, the Dr. You gained physical and biological (and photobiological) techniques. To determine the physical properties of the compounds, the PI learned methods to measure the quantum yields of fluorescence using a fluorimeter and singlet oxygen using a luminometer. For the biological evaluations, the Dr. You also mastered the techniques to determine the cellular uptake of the core-modified porphyrins in cells, to investigate the sub-cellular localization using fluorescence microscopy, and to detect damage to cytochrome c oxidase both in isolated mitochondria and in whole cell.

Diverse arrays of 21,23-dithiaporphyrins were prepared to investigate the effects of the *meso*-aromatic rings on physical and photobiological properties of the compounds. The variation of the *meso*-aromatic rings focused on their steric and electronic properties as well as the degree of symmetry. New synthetic methods were devised to prepare the compounds having a trimethylphenyl or hydroxyphenyl group at the *meso*-position. Overall, about 25 compounds have been synthesized.

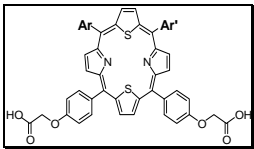
	#	Ar	Ar'	#	Ar	Ar'
	1	2-thienyl	2-thienyl	10	4'-chlorophenyl	4'-chlorophenyl
	2	2-thienyl	phenyl	11	4'-hydroxyphenyl	4'-hydroxyphenyl
	3	mesityl	mesityl	12	4'-methoxyphenyl	4'-methoxyphenyl
	4	mesityl	phenyl	13	4'-dimethyl aminophenyl	4'-dimethyl aminophenyl
	5	4'-tert-butylphenyl	4'-tert-butylphenyl	14	phenyl	phenyl
	6	4'-tert-butylphenyl	phenyl	15	isopropyl	isopropyl
	7	4'-methylphenyl	4'-methylphenyl	16	4'-trifluorophenyl	4'-trifluoromethylphenyl
	8	4'-ethylphenyl	4'-ethylphenyl	17	4'-fluorophenyl	phenyl
	9	4'-butylphenyl	4'-butylphenyl	18	4'-trifluoromethylphenyl	phenyl

Figure 1. The structures of 21,23-dithiaporphyrins prepared during first-year performance.

The physical properties of the compounds were determined such as the absorption maxima, extinction coefficients, quantum yields of fluorescence and singlet-oxygen generation, and $\log D_{7.4}$. Most of the compounds generated singlet oxygen efficiently and absorbed the long-wavelength light ($\sim 700\text{ nm}$) which are important factors for an ideal photosensitizer. The effects of the substituents at *meso*-aromatic ring were minimal on the physical properties except $\log D_{7.4}$. The $\log D_{7.4}$ s, partition between *n*-octanol and phosphate buffer (pH, 7.4), ranged from -0.55 for compound **8** to 0.779 for compound **11**.

The phototoxicity was measured as a biological end point to evaluate the value of the compounds as photosensitizers. Thirteen compounds that expressed potent phototoxic activity, *i.e.*, cell kill > 50% at 0.5 μM with broad band (350-750 nm) light at 1.4mW for 1 hr, were obtained. Dark-toxicity was avoided for these compounds with concentration as high as 10 μM . Compound **2** with two small and different substituents at the *meso*-positions showed the most activity with a 68% cell kill at 0.1 μM with the same intensity of light. More interestingly, in stark contrast to the physical properties, the effects of structural modification at the *meso*-aromatic rings on biological outcome were more dramatic. From the analysis of the structure-activity relationships, the favorable structural features were deduced: 1) the size of *meso*-substituent was inversely correlated with phototoxicity, 2) breaking the symmetry of the molecule increased the activity, and 3) molecular amphiphilicity was important as seen in the case of compound **2**, which lost the activity. *Details were published in article #s 1 and 2 in the outcome section.*

To investigate the underlying mechanism of cell death by core-modified porphyrin **2**, sub-cellular localization, damage of cytochrome *c* oxidase activity, and induction of apoptosis during the cell death were investigated. Irradiation of cells in the presence of 0.2 μM compound **2** resulted in a decrease in cytochrome *c* oxidase activity while dithiaporphyrin **2** at 0.2 μM without irradiation did not affect cytochrome *c* oxidase activity in whole cells. However, compound **2** did not appear to localize in the mitochondria since images of **2**-treated cells by fluorescence microscopy show globular fluorescence inconsistent with mitochondrial localization. Photosensitizer **2** re-localized following irradiation as shown by time-dependent localization using fluorescence microscopy. Interestingly, the dynamic induction of apoptosis depends on the incubation time and concentration of the sensitizer (Figure 2). The production of nucleosomes, which is an indicator of the apoptotic process, reached a maximum with longer incubation (24 hr) with and at appropriate concentration of compound **2** (0.2 μM). We postulate that there are target sites inside cells which can be targeted to trigger the apoptotic pathway by photodynamic treatment with compound **2**. *Details were published in article # 3 in the outcome section.*

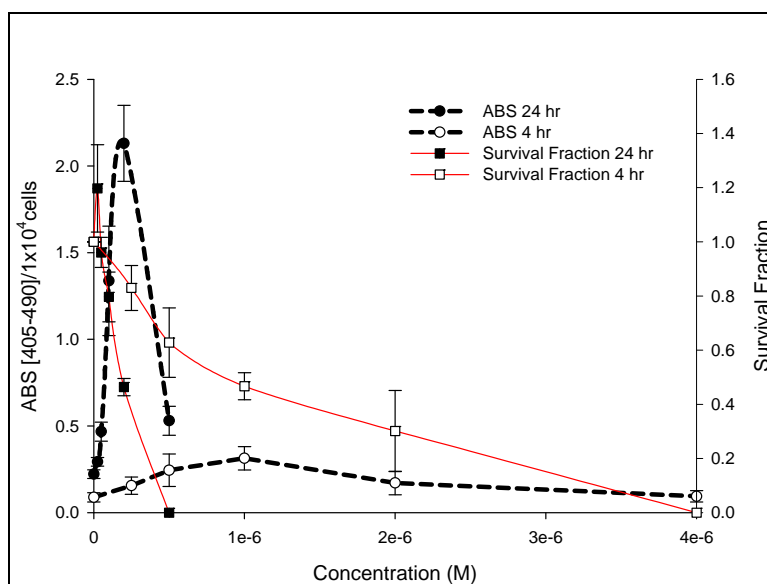


Figure 2. Cell death and detection of nucleosomes in apoptotic process

Second Year

In the second year, the research had been focused on 1) quantitative structure-activity relationships (QSAR) of porphyrins, 2) measurement of binding of PBR, 3) establishment of synthetic methods for novel structure of core-modified porphyrins, and 4) establishment of new synthetic methods for novel structures and preparation of them based on the methods.

QSAR of porphyrins in phototoxicity

QSAR was performed to analyze the effects of structural properties of core-modified porphyrins on phototoxicity (EC_{50}). The structural properties, so called molecular descriptors, of core-modified porphyrins were calculated by the computational methods using Sybyl or modules in the website of Molinspiration. All the calculations were carried out as all ionized form for the sulfonates and both ionized

and unionized forms for carboxylic acids. The correlations between calculated descriptors and measured phototoxicity were determined and expressed in the mathematical models as either simple linear equations or three-dimensional models. From this QSAR analysis, we could tell the important molecular features of core-modified porphyrins for good phototoxicity and use this model in designing new structures.

To achieve a more through analysis of the relationships of structure of core-modified porphyrins with phototoxicity, we included the core-modified porphyrins previously prepared in our laboratory (Fig.1). In general, the calculated lipophilicity of the compounds was the most important molecular property in phototoxicity. MiLogP, calculated logP, showed the strongest correlation with phototoxicity among the descriptors including MW (molecular weight), VOL (molecular volume), AREA (molecular area), and PSA (polar surface area). MiLogP seems to be even more important than physicochemical properties such as ExCoff (excitation coefficient), QYO (quantum yield of singlet oxygen), and LogD7.4, which were experimentally measured. The relationships are expressed as follow and shown in Figure 1a.

$$\text{Log (1/EC}_{50}) = 0.31 \cdot \text{MiLogP} + 3.04, R_2 = 0.71 \text{ (- cp 22) when COOH (Fig. 1a)}$$

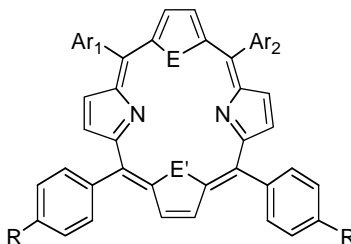
$$\text{Log (1/EC}_{50}) = 0.36 \cdot \text{MiLogP} + 2.83, R_2 = 0.58 \text{ (- cp 22) when COONa}$$

The compounds with higher MiLogP are more potent in phototoxicity, which is consistent with our previous qualitative SAR analyses: EC_{50} : $4 \times \text{SO}_3\text{Na} < 2 \times \text{SO}_3\text{Na} < 2\text{COOH}$ and $4 \times \text{COOH} \sim 3 \times \text{COOH} < 2 \times \text{COOH}$.^{5, 12}

However, there is a group of compounds which shows a different correlation from the whole set of the compounds in red circle in Figure 1a. These compounds are core-modified porphyrins having two carboxylic acids at one side of the molecular structures (compounds 1~20). To examine the QSAR in detail among these compounds, the relationships of steric and electronic descriptors with phototoxicity were analyzed. Of the molecular descriptors, one of the steric parameters, MA (molecular area), demonstrated a very strong correlation with phototoxicity (Fig. 1b). On the other hand, an electronic parameter, PC (point charge at p-carbon at meso phenyl rings) did not show any correlation with phototoxicity.

$$\text{EC}_{50} = 0.003 \cdot \text{MA} - 3.64, R_2 = 0.68 \text{ (Fig. 1b)}$$

Table 1. Data for the QSAR analysis: structures, Phototoxicity, and MiLog P of the core-modified porphyrins



Compd	E1, E2	Ar ₁	Ar ₂	R	EC ₅₀ (M)	M. Area	MiLog P
1	S, S	Phenyl (Ph)	Ph	OCH ₂ COOH	1.5E-07	1258.9	10.805
2	S, S	2,4,5-tri-CH ₃ -Ph	Ph	OCH ₂ COOH	9.0E-08	1367.6	11.235
3	S, S	4-CH ₃ (CH ₂) ₃ -Ph	4-CH ₃ (CH ₂) ₃ -Ph	OCH ₂ COOH	1.0E-06	1524.9	11.786
4	S, S	4-C ₆ H ₆ -Ph	4-C ₆ H ₆ -Ph	OCH ₂ COOH	1.0E-06	1550.7	11.762
5	S, S	4-F-Ph	4-F-Ph	OCH ₂ COOH	2.7E-07	1271.9	10.941
6	S, S	4-F-Ph	Ph	OCH ₂ COOH	8.0E-08	1257.6	10.875
7	S, S	4-Cl-Ph	4-Cl-Ph	OCH ₂ COOH	5.5E-07	1295.5	11.279
8	S, S	4-CF ₃ -Ph	4-CF ₃ -Ph	OCH ₂ COOH	3.3E-07	1366.1	11.393
9	S, S	4-CF ₃ -Ph	Ph	OCH ₂ COOH	2.6E-07	1309.9	11.142
10	S, S	4-CH ₃ O-Ph	4-CH ₃ O-Ph	OCH ₂ COOH	5.6E-07	1350.1	10.854
11	S, S	4-(CH ₃) ₂ N-Ph	4-(CH ₃) ₂ N-Ph	OCH ₂ COOH	2.4E-07	1430.9	10.892
12	S, S	thiophenyl	thiophenyl	OCH ₂ COOH	1.1E-07	1245.8	10.59
13	S, S	4-OH-Ph	4-OH-Ph	OCH ₂ COOH	2.0E-06	1275.5	10.241
14	S, S	thiophenyl	Ph	OCH ₂ COOH	8.0E-08	1251.8	10.703
15	S, S	4-CH ₃ -Ph	4-CH ₃ -Ph	OCH ₂ COOH	1.3E-07	1333.9	11.142

16	S, S	4-CH ₃ CH ₂ -Ph	4-CH ₃ CH ₂ -Ph	OCH ₂ COOH	6.5E-07	1403.6	11.403
17	S, S	4-(CH ₃) ₂ CH-Ph	4-(CH ₃) ₂ CH-Ph	OCH ₂ COOH	1.0E-06	1445.4	11.66
18	S, S	4-(CH ₃) ₃ C-Ph	4-(CH ₃) ₃ C-Ph	OCH ₂ COOH	8.6E-07	1477.3	11.731
19	S, S	4-(CH ₃) ₃ C-Ph	Ph	OCH ₂ COOH	3.0E-07	1360.6	11.372
20	S, S	2,4,5-tri-CH ₃ -Ph	2,4,5-tri-CH ₃ -Ph	OCH ₂ COOH	3.4E-07	1360.8	11.535
21	NH, NH	4-SO ₃ Na-Ph	4-SO ₃ Na-Ph	SO ₃ Na	7.2E-05	-	4.481
22	S, S	4-CF ₃ -Ph	4-CF ₃ -Ph	SO ₃ Na	1.0E-04	1289	8.16
23	S, S	4-(CH ₃) ₂ N-Ph	4-(CH ₃) ₂ N-Ph	SO ₃ Na	6.4E-07	1345.7	8.573
24	S, S	1-SO ₃ Na-4-CH ₃ -Ph	1-SO ₃ Na-4-CH ₃ -Ph	SO ₃ Na	1.2E-05	1287.3	6.723
25	S, S	4-SO ₃ Na-Ph	4-SO ₃ Na-Ph	SO ₃ Na	3.0E-05	1303.3	5.97
26	S, NH	4-SO ₃ Na-Ph	4-SO ₃ Na-Ph	SO ₃ Na	1.0E-04	1301.8	5.225
27	S, S	4-F-Ph	4-F-Ph	SO ₃ Na	1.6E-06	1184.7	8.696

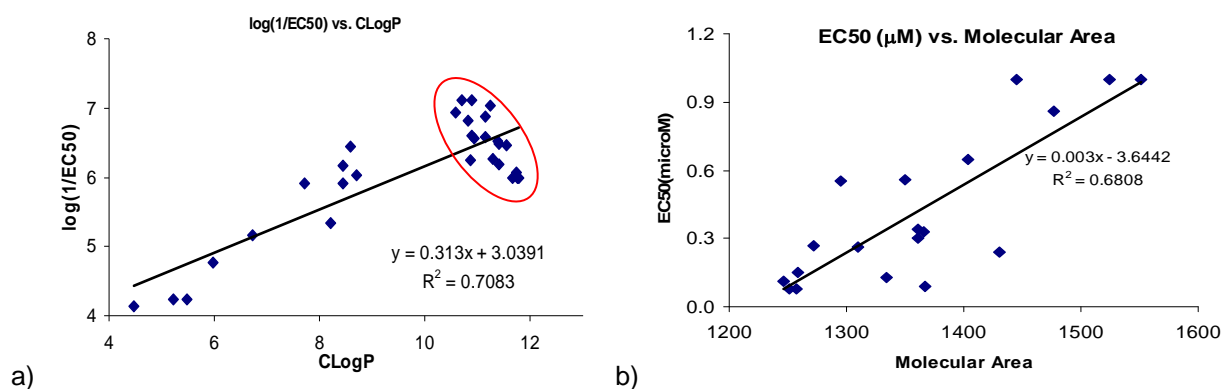


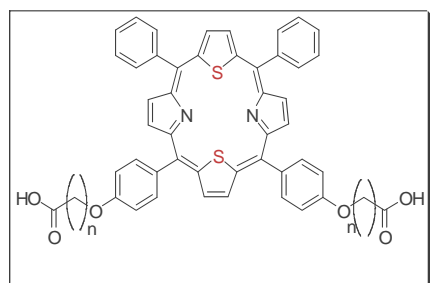
Figure 1. Correlations between a) pED_{50} and $MiLog P$ from compound 1 - 27, b) EC_{50} and Molecular Area for compounds 1 - 20.

Binding of core-modified porphyrins to PBR

Different from our hypothesis, the most potent core-modified porphyrin, compound 2, did not seem to specifically bind to PBR in mitochondria. We could not detect any specific binding of compound 2 to PBR in [³H] PK11195 binding studies in live cells using R3230AC cells. In addition, the image of cellular localization of compound 14 did not show specific localization in mitochondria. We are planning to explore sub-cellular localization of compound 14.

Synthetic methods for novel structures and preparation of new compounds

The modification of new compounds was focused on the unexplored part of core-modified porphyrins. The first set of compounds has different chain lengths between *meso*-phenyl and carboxylic acid groups. The compounds have 1, 3, 4, 5, 6, 10 methylenes, respectively. Interestingly, phototoxicity of the compounds was reversely dependent on the chain length: the shorter of the chain length, the more potent in phototoxicity. It is hypothesized that if the chain length is getting longer, the lipophilicity of the compounds may become too high. Thus, the core-modified porphyrins form more tight aggregates which are unfavorable for biological activity.



compd	no. of CH ₂	$EC_{50} (\mu M)$	$\lambda_{max} (nm)$	$\epsilon (x 10^3 M^{-1} cm^{-1})$
1	1	0.15	435	314
28	3	0.14	438	224
29	4	0.42	438	157
30	5	1.63	438	110
31	6	> 10	438	91
32	10	> 10	438	176

Table 2. Structures of new core-modified porphyrins with various chain length and phototoxicity of them.

The next set of compounds have new structural features compared to the compounds prepared in the first year: 1) core-modified porphyrins with mono functional groups having either carboxylic acid or sulfonate group, 2) chlorine-type dithiaporphyrins with diols in the porphyrin core, and 3) core-modified porphyrins without two *meso*-aryl groups. The core-modified porphyrins with mono-functional group were synthesized based on our previous method.¹³ The chlorine-type dithiaporphyrins were made by oxidation with OsO₄, which gave compound of *syn*-diols.¹⁴ To make the core-modified porphyrins without two *meso*-aryl groups, new diols compound was prepared through a novel intermediate.

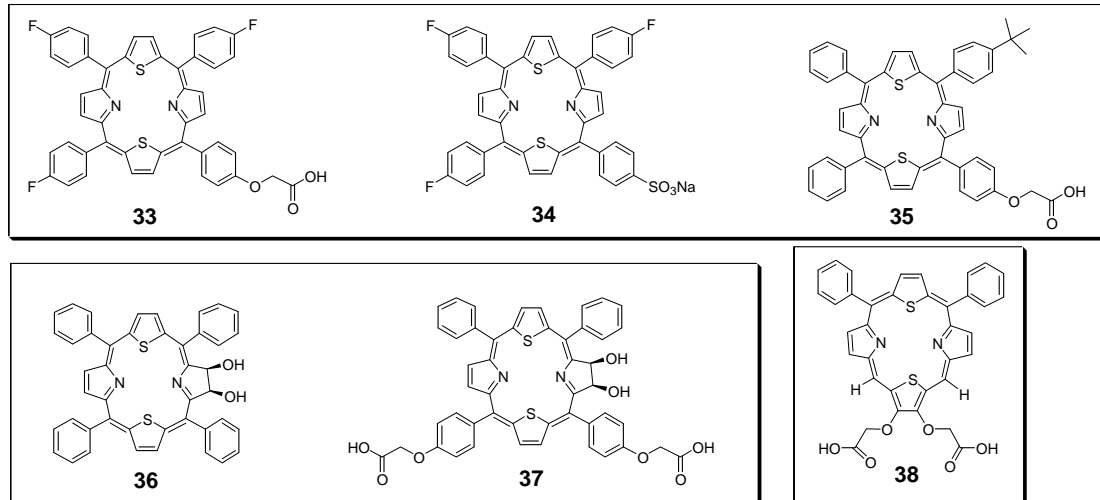


Figure 3. Structures of novel compounds prepared during the second year

Third Year

Work initiated in the past year is ongoing. A series of carboxylic acid-substituted dithiaporphyrins was prepared with different length aliphatic spacers between porphyrin and acid. In a collaborative study with Prof. Benny Ehrenberg at Bar Ilan University in Israel, we found that the efficiency of photooxidizing a membrane-residing singlet oxygen target decreases as the side chains become longer. We suspect that with these large molecules, when their carboxylates are anchored at the lipid:water interface, the tetrapyrrole is in fact closer to the other, opposite, side of the bilayer. This makes these molecules interesting and different from all the others that have been examined in the literature. Conclusions regarding the location of these materials in the bilayer await the synthesis/purchase of phospholipids that are tagged with fluorophores at their heads.

The structures of two derivatives were determined unambiguously by x-ray crystallography including the structure of a *cis*-ABCC *meso*-substituted derivative and the structure of a *cis*-AB disubstituted derivative. Details of these crystal structures are contained in the appendix in the J. Porphyrins Phthalocyanines article (article # 4). The role of the dithiaporphyrins in inducing apoptosis was determined. This work is summarized in the appendix in the J. Photochem. Photobiol. B article (article # 3).

Fourth Year

Due to the relocation of Dr. You, this project was extended to the fourth year without request of further costs.

We used a series of analogues of **1** (compounds **28-32**) as potential photosensitizers for photodynamic therapy (PDT). The photosensitizers differ in the length of the side chains that bind the carboxyl to the phenol at positions 10 and 15 of the thiaporphyrin. The structural changes have almost no effect on the excitation/emission spectra with respect to compound **1**'s spectra or on singlet oxygen generation in MeOH. All of the photosensitizers have a very high, close to 1.00, singlet oxygen quantum yield in MeOH. On the contrary, singlet oxygen generation in liposomes was considerably affected by the structural change in the photosensitizers. The photosensitizers possessing short side chains (one and three carbons) showed high quantum yields of around 0.7, whereas the photosensitizers possessing longer side chains showed smaller quantum yield, down to 0.14 for compound **32** (possessing side-chain length of 10 carbons), all at 1 μ M. Moreover a self-quenching process of singlet oxygen was observed, and the quantum yield decreased as the photosensitizer's concentration increased. We measured the binding constant of **1** to liposomes and found $K_b = 23.3 (1.6 \text{ (mg/mL)})^{-1}$. All the other photosensitizers with longer side chains exhibited very slow binding to liposomes, which prevented us from assessing their K_b 's. We carried out fluorescence resonance energy transfer (FRET) measurements to determine the relative

depth in which each photosensitizer is intercalated in the liposome bilayer. We found that the longer the side chain the deeper the photosensitizer core is embedded in the bilayer. This finding suggests that the photosensitizers are bound to the bilayer with their acid ends close to the aqueous medium interface and their core inside the bilayer. We performed PDT with the dithiaporphyrins on U937 cells and R3230AC cells. We found that the dark toxicity of the photosensitizers with the longer side chain (**32**, **31**, **30**) is significantly higher than the dark toxicity of sensitizers with shorter side chains (**1**, **28**, **29**). Phototoxicity measurements showed the opposite direction; the photosensitizers with shorter side chains were found to be more phototoxic than those with longer side chains. These differences are attributed to the relationship between diffusion and endocytosis in each photosensitizer, which determines the location of the photosensitizer in the cell and hence its phototoxicity. *Details of this study were published article # 5 in the outcome section.*

Thiaporphyrins **33–38** were studied as analogues of **1** and 5,10, 20-triphenyl-15-[4-(carboxymethyleneoxy)-phenyl]-21,23- dithiaporphyrin (**39**) to examine the effect of structural modifications: substituent changes in meso aryl groups of dithiaporphyrins with one water-solubilizing group (**33–35** and **39**), dihydroxylation of a pyrrole double bond and reduction to dihydroxychlorins (**36** and **37**), and the removal of two meso aryl groups to give unsubstituted meso positions (**38**). The impact of these structural modifications was measured in both physicochemical (UV spectra, generation of singlet oxygen, lipophilicity, and aggregate formation) and biological properties (dark toxicity and phototoxicity, cellular uptake, and subcellular localization). Mono-functionalized porphyrins had much higher lipophilicity than di-functionalized porphyrin **1** and, consequently, formed more aggregates in aqueous media. The formation of aggregates might lower the efficiency of lipophilic porphyrins as photosensitizers. Interestingly, dihydroxylation of a core pyrrole group in the dithiaporphyrin core did not affect either the absorption spectrum or the efficiency for generating singlet oxygen. The phototoxicity of dihydroxydithiachlorins mainly depended on their intracellular uptake. The potent phototoxicity of **6**, $IC_{50} = 0.18 \mu M$, was attributed to the extraordinarily high uptake. The intracellular uptake of **36** was about 7.6 times higher than **1**. In contrast, thiaporphyrin **38** with only two meso aryl groups was less effective as a photosensitizer, perhaps due to poorer uptake and a lower quantum yield for the generation of singlet oxygen. *Details of this study were published article # 7 in the outcome section.*

Key Research Accomplishments

Training: Dr. You (former PI) acquired knowledge and skills of photodynamic therapy, covering all aspects of chemical, photophysical, and biological aspects. He obtained a tenured-track faculty position in the Department of Chemistry and Biochemistry at the South Dakota State University.

Research accomplishments: 1) Thirty seven new core modified porphyrins were successfully prepared. 2) QSAR of the core-modified porphyrins was established. 3) Cell death mechanism (apoptosis) by PDT with this type of photosensitizers was confirmed, which was dependent on experimental conditions.

Reportable Outcomes

Publications

1. You, Y.; Gibson, S. L.; Hilf, R.; Ohulchanskyy, T. Y.; Detty, M. R. Core-modified porphyrins. Part 4: Steric effects on photophysical and biological properties in vitro. *Bioorg Med Chem* 2005, 13, 2235-2251.
2. You, Y.; Gibson, S. L.; Detty, M. R. Core-modified porphyrins. Part 5: Electronic effects on photophysical and biological properties in vitro. *Bioorg Med Chem* 2005, 13, 5968-5980.
3. You, Y.; Gibson, S. L.; Detty, M. R. Phototoxicity of a core-modified porphyrin and induction of apoptosis. *Journal of Photochemistry and Photobiology B: Biology* 2006, 85, 155-162.
4. You, Y.; Daniels, T. S.; Dominiak, P. M.; Detty, M. R. Synthesis, spectral data, and crystal structure of two novel substitution patterns in dithiaporphyrins. *Journal of Porphyrins and Phthalocyanines* 2007, 11, 1-8.
5. Ngen, E. J.; Daniels, T. S.; Murthy, S. R.; Detty, M. R.; You, Y. Core-modified porphyrins. Part 6: Effects of lipophilicity and core structures on physicochemical and biological properties in vitro. *Bioorg Med Chem* 2008, 16, 3171-3183.

6. Minnes, M; Weitman, H.; You, Y.; Detty, M.R.; Ehrenberg, B. Dithiaporphyrin derivatives as photosensitizers in membranes and cells. *Journal of Physical Chemistry B* 2008, 112, 3268-3276.

Presentations

1. You, Y.; Gibson, S. L.; Hilf R.; Detty, M. R. Study of New Core-modified Porphyrins as Photosensitizers for Photodynamic Cancer Therapy, The 229th ACS National Meeting, March 13-17, 2005, San Diego, CA.
2. You, Y.; Gibson, S. L.; Hilf R.; Detty, M. R. Structure-Activity Relationship of 21,23-Core-Modified Porphyrins for Photodynamic Therapy of Cancer. The 4th Era of Hope meeting for the Department of Defense (DOD) Breast Cancer Research Program (BCRP), June 8-11, 2005, Philadelphia, PA.
3. You, Y.; Gibson S. L.; Hilf R.; Detty, M. R. SAR of new core-modified porphyrins as photosensitizers for photodynamic cancer therapy: electronic effects and importance of aggregation in biological activity. The 230th ACS National Meeting, August 28-September 1, 2005, Washington, DC.
4. Gannon, M. R.; Tomblin, G.; Donnelly, D. J.; Holt, J. J.; You, Y.; Ye, M.; Nygren, C. L.; Detty, M. R. Characterization of the "R" binding site of P-glycoprotein: Using novel chalcogenoxanthylum tetramethylrosamine analogues for the stimulation of ATPase activity. The 232th ACS National Meeting, September 10-14, 2006, San Francisco, CA.
5. Ngen, E. J.; Murthy, M. R.; You, Y. Core- Modified Porphyrins: Effects of Substituents on Photophysical Properties and In Vitro Photodynamic Activity. The 42nd ACS Midwest Regional Meeting, November 7-10, 2007, Kansas City, MO.

Conclusions

Due to this postdoctoral support, Dr. You successfully completed his training and he is now employed as an assistant professor in the Department of Chemistry at South Dakota State University. The results of this study provide generally acceptable guides in designing new photosensitizers. Such extensive QSAR study with a single lead compound was never present.

References

1. Dougherty, T.J. et al. Photodynamic therapy. *J. Natl. Cancer Inst.* **90**, 889-905 (1998)
2. Detty, M. Photosensitizers for the photodynamic therapy of cancer and other diseases. *Expert Opin. Ther. Patents.* **11**, 1849-1860 (2001)
3. Stilts, C.E. et al. Water-soluble, core-modified porphyrins as novel, longer-wavelength-absorbing sensitizers for photodynamic therapy. *J. Med. Chem.* **43**, 2403-2410 (2000)
4. Hilf, D.G. et al. Water-soluble, core-modified porphyrins as novel, longer-wavelength-absorbing sensitizers for photodynamic therapy. II. Effects of core heteroatoms and meso-substituents on biological activity. *J Med Chem* **45**, 449-461 (2002)
5. You, Y., Gibson, S.L., Hilf, R., Ohulchanskyy, T.Y. & Detty, M.R. Core-modified porphyrins. Part 4: Steric effects on photophysical and biological properties in vitro. *Bioorg Med Chem* **13**, 2235-2251 (2005)
6. Furre, I.E. et al. Targeting PBR by hexaminolevulinic-mediated photodynamic therapy induces apoptosis through translocation of apoptosis-inducing factor in human leukemia cells. *Cancer Res* **65**, 11051-11060 (2005)
7. Morris, R.L. et al. The peripheral benzodiazepine receptor in photodynamic therapy with the phthalocyanine photosensitizer Pc 4. *Photochem Photobiol* **75**, 652-661 (2002)
8. Dougherty, T.J. et al. The role of the peripheral benzodiazepine receptor in photodynamic activity of certain pyropheophorbide ether photosensitizers: albumin site II as a surrogate marker for activity. *Photochem Photobiol* **76**, 91-97 (2002)
9. Hardwick, M. et al. Peripheral-type benzodiazepine receptor (PBR) in human breast cancer: correlation of breast cancer cell aggressive phenotype with PBR expression, nuclear localization, and PBR-mediated cell proliferation and nuclear transport of cholesterol. *Cancer Res* **59**, 831-842 (1999)
10. Hardwick, M., Rone, J., Han, Z., Haddad, B. & Papadopoulos, V. Peripheral-type benzodiazepine receptor levels correlate with the ability of human breast cancer MDA-MB-231 cell line to grow in SCID mice. *Int J Cancer* **94**, 322-327 (2001)
11. Hardwick, M., Cavalli, L.R., Barlow, K.D., Haddad, B.R. & Papadopoulos, V. Peripheral-type benzodiazepine receptor (PBR) gene amplification in MDA-MB-231 aggressive breast cancer cells. *Cancer Genet Cytogenet* **139**, 48-51 (2002)

12. You, Y., Gibson, S.L. & Detty, M.R. Core-modified porphyrins. Part 5: Electronic effects on photophysical and biological properties in vitro. *Bioorg Med Chem* **13**, 5968-5980 (2005)
13. You, Y. et al. Water soluble, core-modified porphyrins. 3. Synthesis, photophysical properties, and in vitro studies of photosensitization, uptake, and localization with carboxylic acid-substituted derivatives. *J Med Chem* **46**, 3734-3747 (2003)
14. Lara, K.K., Rinaldo, C.R. & Brückner, C. meso-Tetraaryl-7,8-diol-21,23-dithiachlorins and their pyrrole-modified derivatives: a spectroscopic comparison to their aza-analogues. *Tetrahedron* **61**, 2529-2539 (2005)

Appendices (Other publications were submitted in our previous annual reports)

1. *Bioorg Med Chem* 2008, 16, 3171-3183.
2. *Journal of Physical Chemistry B* 2008, 112, 3268-3276.



Core-modified porphyrins. Part 6: Effects of lipophilicity and core structures on physicochemical and biological properties in vitro

Ethel J. Ngen,^a Thalia S. Daniels,^b Rajesh S. Murthy,^a
Michael R. Detty^b and Youngjae You^{a,*}

^aDepartment of Chemistry and Biochemistry, South Dakota State University, Brookings, SD 57007, USA

^bDepartment of Chemistry, University at Buffalo, The State University of New York, Buffalo, NY 14260, USA

Received 30 October 2007; revised 10 December 2007; accepted 11 December 2007

Available online 27 December 2007

Abstract—Thiaporphyrins **2–8** were prepared as analogues of 5,20-diphenyl-10,15-bis[4-(carboxymethyleneoxy)-phenyl]-21,23-dithiaporphyrin (**1**) to examine the effect of structural modifications: substituent changes in meso aryl groups of dithiaporphyrins with one water-solubilizing group (**2–5**), dihydroxylation of a pyrrole double bond and reduction to dihydroxychlorins (**6** and **7**), and the removal of two meso aryl groups to give unsubstituted meso positions (**8**). The impact of these structural modifications was measured in both physicochemical (UV spectra, generation of singlet oxygen, lipophilicity, and aggregate formation) and biological properties (dark toxicity and phototoxicity, cellular uptake, and subcellular localization). Mono-functionalized porphyrins had much higher lipophilicity than di-functionalized porphyrin **1** and, consequently, formed more aggregates in aqueous media. The formation of aggregates might lower the efficiency of lipophilic porphyrins as photosensitizers. Interestingly, dihydroxylation of a core pyrrole group in the dithiaporphyrin core did not affect either the absorption spectrum or the efficiency for generating singlet oxygen. The phototoxicity of dihydroxydithiachlorins mainly depended on their intracellular uptake. The potent phototoxicity of **6**, $IC_{50} = 0.18 \mu M$, was attributed to the extraordinarily high uptake. The intracellular uptake of **6** was about 7.6 times higher than **1**. In contrast, thiaporphyrin **8** with only two meso aryl groups was less effective as a photosensitizer, perhaps due to poorer uptake and a lower quantum yield for the generation of singlet oxygen.

© 2007 Elsevier Ltd. All rights reserved.

1. Introduction

Photodynamic therapy (PDT) offers a great opportunity to reduce severe side effects and enhance selectivity in cancer treatments due to its unique mechanism of action.^{1,2} The expression of biological activity in PDT is derived from the combined effect of three components: a photosensitizer, light, and oxygen. Excited-state photosensitizers generate reactive oxygen species by the transfer of energy to produce singlet oxygen or by the transfer of electrons to produce superoxide, hydrogen peroxide, or hydroxyl radicals. Therefore, although photosensitizers are generally administered systemically, damage by PDT occurs only near/around the areas irradiated by the light. Although Photofrin[®] has been effective as a first-generation photosensitizer, it has several

problems.^{3,4} Physically, Photofrin[®] is a mixture of compounds, which makes pharmacological evaluation difficult and causes problems in terms of reproducibility in its preparation. In addition, some patients suffer long-term skin photosensitization following treatment with Photofrin[®]. Furthermore, Photofrin[®] is only weakly absorbing at its absorption maximum (~ 630 nm), which limits the photoefficiency of treatment and its absorption maximum limits the depth of penetration of activating light.

Core-modified porphyrins, in particular dithiaporphyrins, have several advantages: flexibility in synthesis, preparation in high purity, absorption at longer wavelengths (band I absorption maxima of ~ 700 nm), and high photostability.⁵ In an effort to develop second-generation, dithiaporphyrin photosensitizers, we synthesized numerous core-modified porphyrins and studied the relationship between their structure and their phototoxicity.^{5–11} Dithiaporphyrins with two carboxylic acid groups were found to be more efficient photosensitizers than dithiaporphyrins with one, three, and four carbox-

Keywords: Core-modified porphyrin; Thiaporphyrin; Photodynamic therapy; Anticancer therapy; SAR.

* Corresponding author. Tel.: +1 605 688 6905; fax: +1 605 688 6364; e-mail: youngjae.you@sdstate.edu

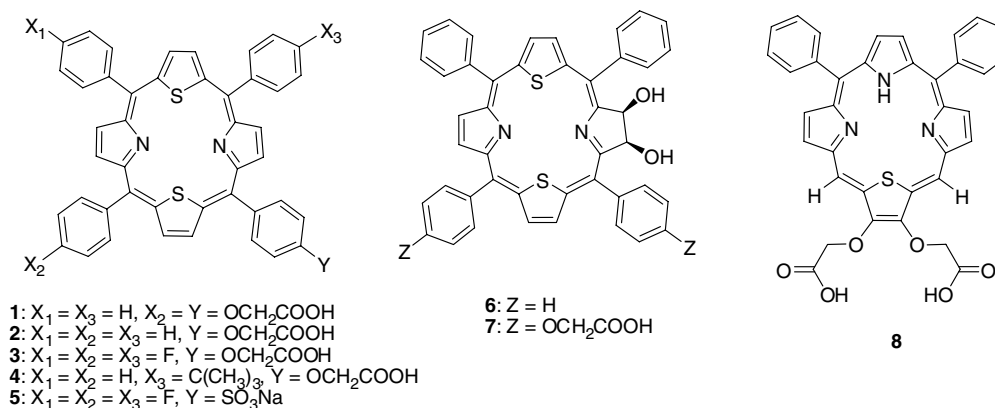


Figure 1. Structures of 21-mono- or 21,23-dithiaporphyrins.

ylic acid groups.⁸ Among dithiaporphyrins with two carboxylic acid groups, steric effects at the meso-aryl substituents were more determinant of phototoxicity than electronic effects at the meso-aryl groups and a preference was noted for smaller substituents and two different meso substituents.^{5,9}

In this report, we extend our SAR study to mono-functionalized dithiaporphyrins 2–5, dihydroxydithiachlorins 6 and 7, and monothiaporphyrin 8 bearing only two meso-aryl groups (Fig. 1). We describe the syntheses of 2–8 as well as the measurement of their cellular uptake and phototoxicity. In order to elucidate the determining factors for phototoxicity, the absorption spectra, relative yields for the generation of singlet oxygen, the lipophilicity ($\log D_{7.4}$), the aggregation tendency, and sites of sub-cellular localization were determined.

2. Results and discussion

2.1. Chemistry

Compounds 1 and 2 were prepared as described in our earlier work.⁸ The syntheses of 3–8 used methods that we developed to construct asymmetric core-modified porphyrins.

2.1.1. Synthesis of mono-functionalized core-modified porphyrins. Trifluorinated mono-carboxylic acid dithiaporphyrin, 3, was prepared based on previous synthetic methods used for the preparation of asymmetric dithiaporphyrins.⁸ Compound 9 was synthesized from thiophene and 4-fluorobenzaldehyde in 46% isolated yield. After protection of the hydroxyl group of 9 with *tert*-butyldimethylsilyl chloride (TBSCl), the dihydroxy compound 11 was prepared from 9 and *p*-anisaldehyde in 74% yield after deprotection of the TBS group with 1 M TBAF. Condensation of 11 with 2,5-bis[1-(4-fluorophenyl)-1-pyrrolomethyl]thiophene 12 afforded the dithiaporphyrin 13 in 8.5% isolated yield. Demethylation of 13 with BBr_3 gave 14 in 82% yield. The final product, 3, was obtained after alkylation with ethyl bromoac-

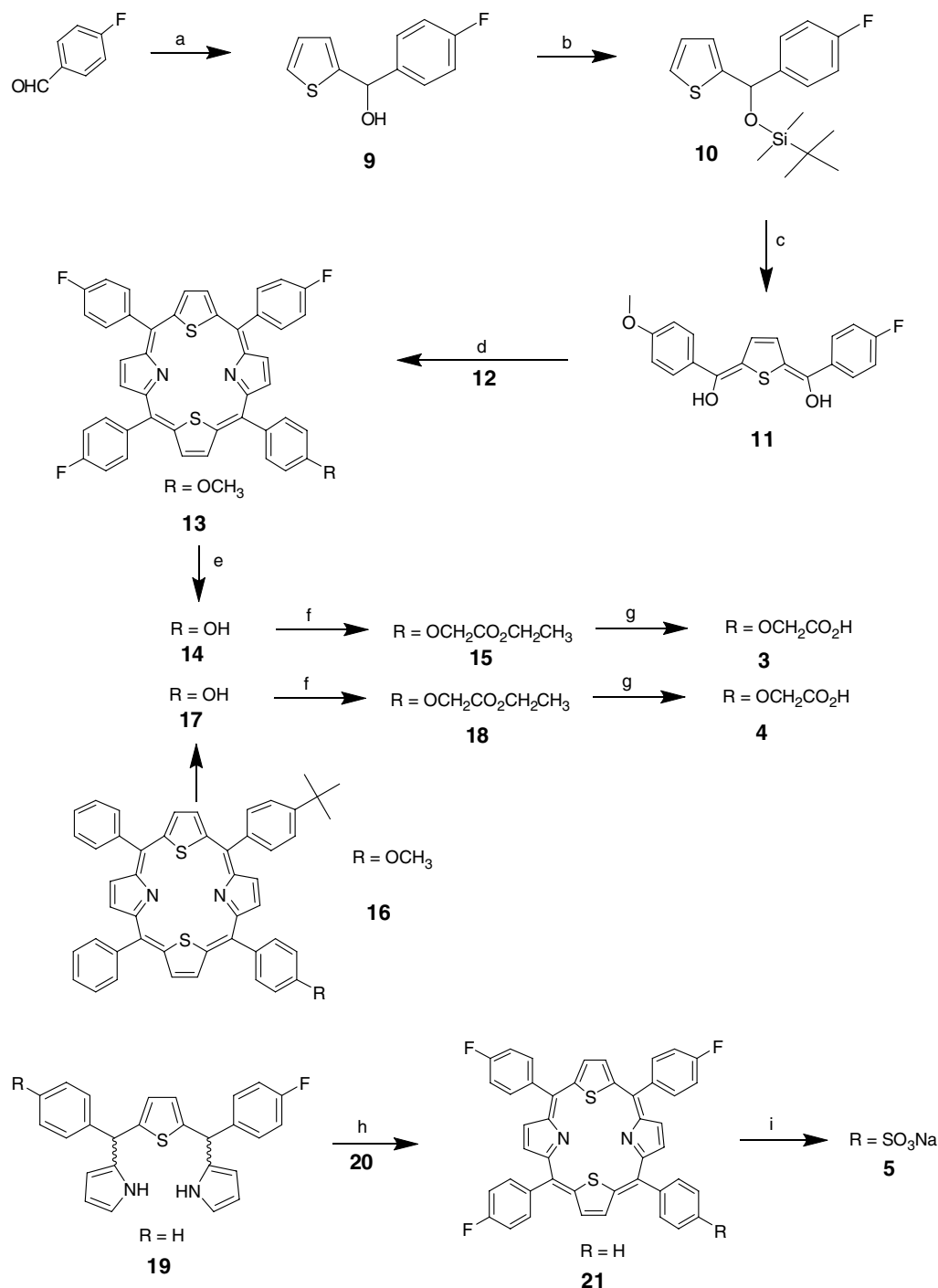
tate to give 15 followed by saponification of the ethyl ester. Dithiaporphyrin 4 was prepared using similar chemistry to that used for the preparation of 3 starting with methoxy porphyrin 16.¹⁰ Compound 21 was obtained in 14% isolated yield through the condensation reaction of 19 and 2,5-bis[1-(4-fluorophenyl)-1-hydroxymethyl]thiophene 20. Sulfonation of the meso-phenyl group of 21 afforded 5 in 50% isolated yield (Scheme 1).

2.1.2. Synthesis of dihydroxydithiachlorins. Dihydroxydithiachlorins, 6 and 7, were synthesized via oxidation of a pyrrole double bond with OsO_4 to give *syn*-dihydroxylation.¹² The precursor dithiaporphyrins, 22 and 23, were prepared using previously reported chemistry.^{6,8} 7,8-Dihydroxydithiaporphyrins 6 and 24 were prepared by oxidation with OsO_4 in a solvent mixture of chloroform and 1% pyridine, in 34% and 19% yields, respectively. Saponification of the esters in 24 gave dihydroxydithiaporphyrin 7 with two carboxylic acids in 75% yield (Scheme 2).

2.1.3. Synthesis of core-modified porphyrin 8 with two meso-aryl groups and two unsubstituted meso positions. Core-modified porphyrin 8 with two unsubstituted meso-positions was prepared in several steps from dimethoxy thiophene 25.¹³ Initial condensation of 25 with benzaldehyde and pyrrole in the presence of *p*-toluenesulfonic acid and TCBQ gave 27 in 6% isolated yield. Demethylation of 27 with BBr_3 , alkylation of the resulting diol 28 with ethyl bromoacetate, and saponification of the two ester groups of 29 provided carboxylic acid 8 (Scheme 3).

2.2. Photophysical properties

2.2.1. Absorption spectra. Mono-functionalized dithiaporphyrins 2–5 absorb light at wavelengths similar to those reported for other dithiaporphyrins^{6–11} with band I maxima near 700 nm. Dihydroxydithiachlorins 6 and 7 have band I maxima at 698 nm consistent with reported data for other dihydroxydithiachlorins (Table 1).¹² In contrast, thiaporphyrin 8 with two unsubstituted meso positions has a band I absorption maximum at 665 nm. The shorter wavelength is presumably due to

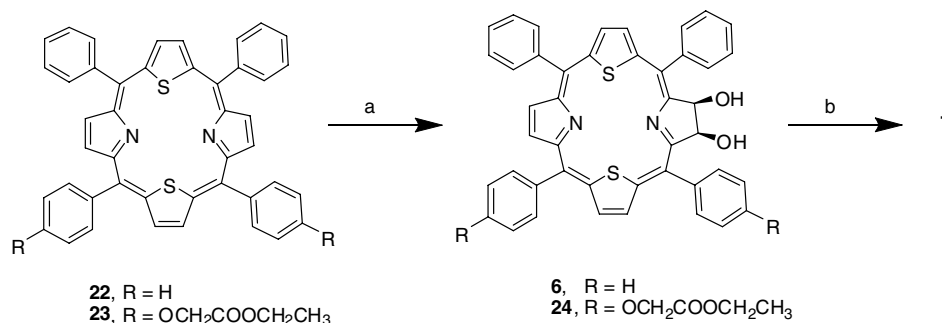


Scheme 1. Reagents: (a) i—1 equiv *n*-BuLi, ii—1 equiv thiophene; (b) TBSCl, DMAP, Et₃N; (c) i—1 equiv *n*-BuLi, ii—1 equiv 4-methoxybenzaldehyde, iii—aqueous HCl; (d) **12**, TCBQ, TsOH·H₂O, CH₂Cl₂; (e) BBr₃, CH₂Cl₂; (f) BrCH₂CO₂Et, K₂CO₃, acetone; (g) NaOH, aqueous THF; (h) **20**, TCBQ, TsOH·H₂O, CH₂Cl₂; (i) concd H₂SO₄.

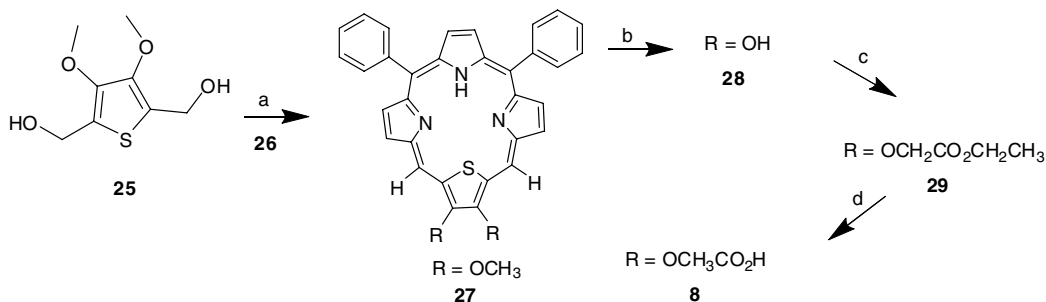
the incorporation of only one sulfur atom in the core and the lack of two meso-aryl groups.¹⁴

2.2.2. Generation of singlet oxygen. To estimate the relative rates of singlet oxygen in core-modified porphyrins **1–8**, we measured the decrease in 1,3-diphenylisobenzofuran (DPBF) absorbance as DPBF reacted with singlet oxygen generated by irradiation of the core-modified porphyrin. A tetrahydrofuran (THF)

solution of DPBF (90 μM) and core-modified porphyrin (1 μM) was irradiated with 3 mW/cm² of the water-filtered halogen source (400–850 nm) for 10 min (1.8 J/cm²).¹⁵ THF was used as a solvent to avoid potential problems from aggregation. The percentages of oxidized DPBF by each porphyrin are summarized in Table 2. Consistent with our previous studies,^{5,8,9} dithiaporphyrins **1–5** were excellent singlet oxygen generators. Interestingly, dihydroxydithiachlorins **6** and **7** generated



Scheme 2. Reagents: (a) OsO_4 , $\text{CHCl}_3/\text{pyridine}$ (100:1), H_2S , NaOH ; (b) NaOH , aqueous THF.



Scheme 3. Reagents: (a) 2,5-bis(2-phenyl-1-hydroxymethyl)thiophenepyrrole (**26**), TCBQ, $\text{TsOH}\cdot\text{H}_2\text{O}$, CH_2Cl_2 ; (b) BBR_3 , CH_2Cl_2 ; (c) $\text{BrCH}_2\text{CO}_2\text{Et}$; (d) NaOH , aqueous THF.

Table 1. UV–vis–near-IR band maxima and molar absorptivities for core-modified porphyrins in tetrahydrofuran^a

Compound	Soret band	Band IV	Band III	Band II	Band I
1	438 (119)	516 (20.8)	547 (11.1)	633 (2.2)	698 (6.0)
2	438 (205)	516 (25.2)	547 (9.8)	633 (2.2)	698 (6.1)
3	442 (185)	520 (24.8)	548 (10.7)	635 (2.6)	699 (6.1)
4	439 (200)	513 (26.3)	548 (10.3)	634 (2.1)	698 (5.8)
5^b	436 (132)	512 (20.3)	544 (5.6)	631 (1.5)	694 (3.2)
6	438 (154)	516 (22.8)	547 (3.3)	633 (10.9)	698 (4.9)
7	438 (108)	516 (18.7)	547 (15.0)	633 (3.6)	698 (8.6)
8	428 (70.9)	505 (21.9)	561 (3.0)	604 (5.2)	665 (2.9)

^a λ_{max} nm ($\epsilon \times 10^3 \text{ M}^{-1} \text{ cm}^{-1}$).

^b In MeOH.

Table 2. Percentiles of oxidized DPBF by the irradiation with porphyrins and *n*-octanol/water partition coefficients in pH 7.4 phosphate buffer

Compound	Oxidized DPBF (%)	$\log D_{7.4}$
1	68	0.1
2	78	1.6
3	75	1.8
4	75	>2
5	64	0.8
6	78	>2
7	62	−0.5
8	48	0.8

singlet oxygen, 78% and 62% oxidation, respectively, as effectively as dithiaporphyrins **1–5**. The mono-thiaporphyrin **8**, with two unsubstituted meso-positions, was less efficient than the others for the generation of singlet oxygen with only 48% oxidized DPBF.

2.2.3. *n*-Octanol/pH 7.4 buffer partition coefficients. The lipophilicity of a molecule is important not only in cellular uptake, but also in the determination of water solubility, which is closely related to the tendency to form aggregates. This is especially true for porphyrins. Partition coefficients of porphyrins **1–8** were determined as $\log D_{7.4}$ using *n*-octanol and pH 7.4 phosphate buffer. Experimental $\log D_{7.4}$ values reflected the effects of substituents at meso-aryl groups except **8**. Monocarboxylic acids **2–4** and monosulfonated porphyrin **5** had higher values of $\log D_{7.4}$ than dicarboxylic acid porphyrin, **1**. Sulfonated porphyrin **5** had a lower value of $\log D_{7.4}$ due to the higher acidity of the sulfonic acid residue relative to the carboxylic acid. Monocarboxylic acid porphyrin **4** with a *tert*-butyl group showed a higher value of $\log D_{7.4}$ than **2**. The hydrophilic effect of the two alcohol substituents of **6** was much smaller than the effect of the two carboxylic acid substituents of **1** ($\log D_{7.4}$ of >2 vs $\log D_{7.4}$ of 0.1). However, the addition of two hydro-

xyl groups in **1** to give dithiachlorin **7** significantly lowered $\log D_{7.4}$ from 0.1 for **1** to -0.5 for **7**. Interestingly, $\log D_{7.4}$ of **8** was higher than that of **1** (0.8 vs 0.1) even though both have two carboxylic acid residue and **8** lacks two aromatic meso substituents.

2.3. Biology

2.3.1. Dark and phototoxicity of core-modified porphyrins toward cultured R3230AC cells. We tested the photodynamic activity of the core-modified porphyrins against R3230AC cells. The porphyrins were added to the cells 24 h before the irradiation with water-filtered halogen light source (3 mW/cm^2 for 1 h, 10.8 J/cm^2). Cell viability was determined by MTT colorimetric assay.¹⁶ The Hill (sigmoid Emax) equation was used to fit the data (Fig. 2) and to calculate values of IC_{50} . Values of IC_{50} ranged from 0.13 to $2.6 \mu\text{M}$: a 20-fold difference between the best and the worst. Dithiachlorin derivative **7** and thiaporphyrin **8** with two unsubstituted meso positions showed much lower potency than the others with values of $\text{IC}_{50} > 2 \mu\text{M}$. Among the mono-functionalized porphyrins, **4** and **5** were less phototoxic than **2** and **3**. Interestingly, dithiachlorin **6** was more phototoxic than derivatives **2–5**, **7**, and **8**, and was similar to **1** in phototoxicity. In dark and light controls, no dark toxicity was observed in R3230AC cells at porphyrin concentrations up to $10 \mu\text{M}$ and no toxicity was observed in R3230AC cells treated with 10.8 J/cm^2 of water-filtered halogen light (data not shown).

2.3.2. Intracellular accumulation of core-modified porphyrins in R3230AC cells. The cellular concentration of the various porphyrins was determined by fluorescence and is expressed in fmole per cell as shown in Figure 3. Cells were treated with $10 \mu\text{M}$ core-modified porphyrin

for 24 h. With the exception of the intracellular concentration of **6**, concentrations of all porphyrins were less than 1 fmole per cell (0.31–0.59 fmole/cell). In particular, the uptake of **7** and **8** was much less than the others, 0.11 and 0.16 fmole/cell, respectively. On the other hand, **6** showed much higher uptake, 4.5 fmole/cell. The uptake of the porphyrins in cells seems to correlate with phototoxicity. The potent activity of **6** is accompanied by the highest uptake (4.5 fmole/cell) among core-modified porphyrins **1–8**. The lower uptake of **7** and **8** also correlates with the low phototoxicity of these two compounds. The relatively low lipophilicity of **7** ($\log D_{7.4}$, -0.5) might make passage through the lipid bilayer of cell membrane difficult. This observation is consistent with our previous results where core-modified porphyrins with three or four carboxylic acids showed much lower uptake.⁸ The lower efficiency of singlet oxygen generation in **8** also contributes to the lower potency of **8** (Table 2). The sulfonated porphyrin **5** showed lower potency than the carboxylated porphyrins, although the uptake (0.30 fmole/cell) was close to the uptake observed with **2** (0.31 fmole/cell) and **3** (0.33 fmole/cell) and singlet oxygen was generated nearly as effectively (64%) as the others (75–78%).

Extraordinarily high uptake of **6** (4.5 fmol/cell) was unexpected because it was highly lipophilic and formed aggregates in the media. Compound **4** also showed high lipophilicity and formed aggregates well, but uptake was much lower (0.46 fmol/cell). Compound **6** might cross cell membrane more readily due to two reasons: (1) it is smaller in size and (2) it does not have flexible hydrophilic functional group, which could interfere the porphyrin's crossing through plasma membrane as both a monomer and an aggregate. However, we do not exclude the possibility that compound **6** forms different

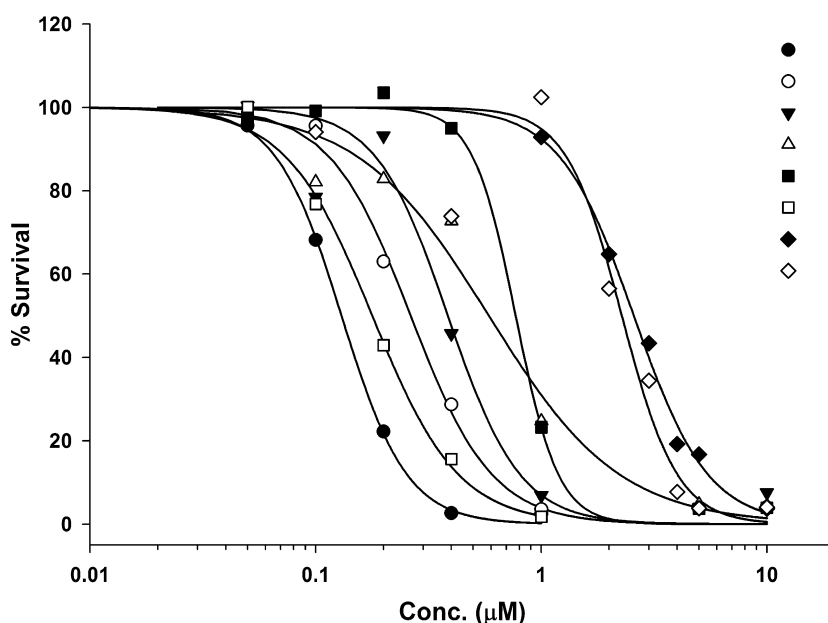


Figure 2. Cell viability of cultured R3230AC cells after photosensitization in the presence of thiaporphyrins **1–8**. Each data point represents the mean of at least 3 separate experiments performed in duplicate and error bars are the SEM. Data are expressed as the surviving fraction of viable cells relative to untreated controls. IC_{50} (μM): **1** (0.13), **2** (0.26), **3** (0.38), **4** (0.59), **5** (0.77), **6** (0.18), **7** (2.57), and **8** (2.28).

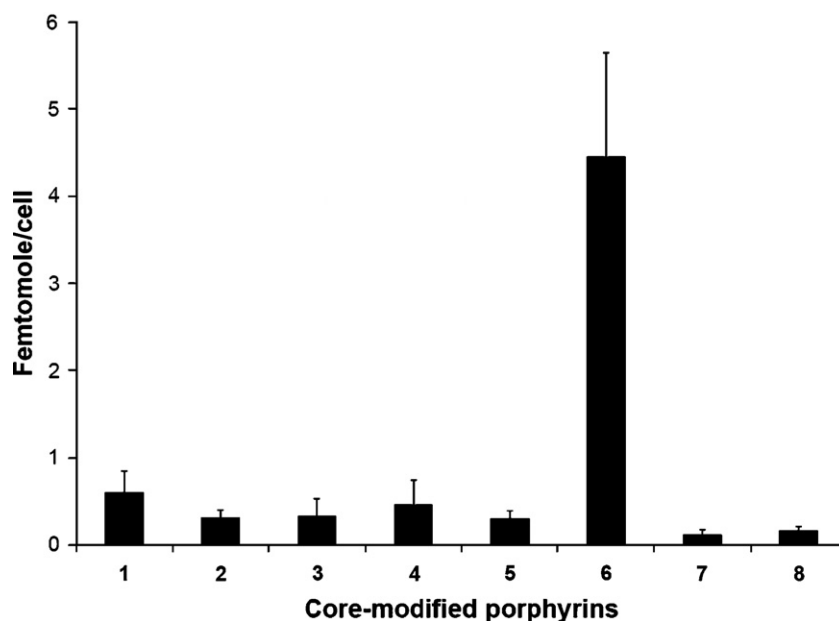


Figure 3. Cellular uptake of thiaporphyrins **1–8** in cultured R3230AC cells. Each bar represents the mean intracellular uptake of each compound incubated with R3230AC cells for 24 h at 1×10^{-5} M. Data are expressed as femtomole porphyrin/cell and error bars are the SEM.

type of aggregates due to the absence of the flexible hydrophilic chain.

2.3.3. Aggregates of core-modified porphyrins in media.

The extent of core-modified porphyrin aggregation in growth medium was indirectly determined by a comparison of their fluorescence yield in medium relative to their fluorescence observed in DMSO (Fig. 4). The loss of fluorescence emission upon aggregation of porphyrins has been reported for both anionic and cationic porphyrins.^{17,18} The decrease in fluorescence of lipophilic porphyrins **2–6** in medium compared to that in DMSO was quite apparent as shown in Figure 4. Fluorescence from the more hydrophilic porphyrins **1**, **7**, and **8** showed little difference between growth medium and DMSO. These data indicate that the lipophilic porphyrins are more prone to form aggregates than hydrophilic porphyrins in medium.

The tendency to aggregate seemed the most striking factor responsible for the lower efficiency of highly lipophilic porphyrins, for example, **4** and **6**. Although the intracellular uptake of **4** (0.46 fmole/cell) was close to that of **1** (0.59 fmole/cell), **1** was about 4.5 times more potent than **4** (IC_{50} , 0.13 μ M vs 0.59 μ M). The IC_{50} of **6** was slightly higher than that of **1** (0.18 vs 0.13 μ M), but the cellular concentration of **6** was 7.6 times higher than that of **1** (4.5 vs 0.59 fmole/cell). On a 'molecule per cell' basis, both **4** and **6** were much less efficient as photosensitizers than **1**. In general, when dyes form aggregates, quantum yields for photophysical processes such as fluorescence emission and singlet oxygen generation are decreased. We suggest that the high tendency of **6** and **4** to form aggregates in media may be mirrored in the cytoplasm causing the lowered phototoxicity of the lipophilic photosensitizers.

2.3.4. Sub-cellular localization of core-modified porphyrin in R3230AC cells.

The site of intracellular localization of the photosensitizer has been suggested to be one of the main factors in determining the efficiency of photodynamic activity.¹⁹ This statement is supported by two observations: (1) the site of localization of the photosensitizers will be the site of cellular damage since the diffusion distance of singlet oxygen is no further than 20 nm in a biological system²⁰ and (2) the sensitivity of organelles to damage by singlet oxygen can be quite different. Photodynamic damage to mitochondria can lead to the induction of apoptosis,^{21–23} which has made mitochondria the premier target of photosensitizers.^{24,25}

In order to discern the subcellular localization of the core-modified porphyrins, R3230AC cells were treated with core-modified porphyrins **1**, **4**, or **6**, or with rhodamine-123 (**Rh-123**), a standard mitochondrial staining dye (Fig. 5).²⁶ R3230AC cells were incubated with 20 μ M of the core-modified porphyrin for 24 h or with 13 μ M **Rh-123** for 30 min and were then washed three times with media to remove residual porphyrin or **Rh-123**. The core-modified porphyrins did not provide the fine, granular fluorescence associated with mitochondrial specificity as shown with **Rh-123** in Figure 5. While all three core-modified porphyrins gave similar fluorescence images, some slight differences were observed. Staining with **4** looked more specific without more diffuse staining area. The core-modified porphyrins did not stain nuclei and, while mitochondria may be stained, the core-modified porphyrins were not specific for mitochondria. These images did not provide conclusive information to explain the differences of the efficiency between hydrophilic core-modified porphyrin, **1**, and lipophilic porphyrins, **4**, **6**.

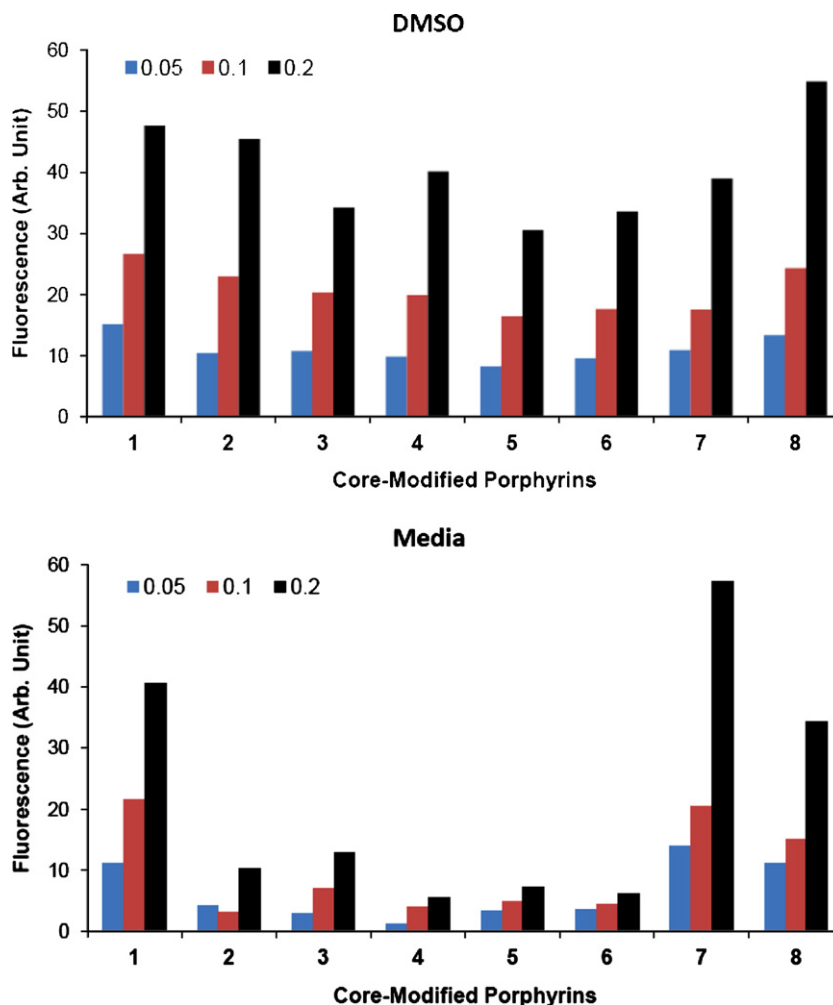


Figure 4. Fluorescence emission from core-modified porphyrins 1–8 in DMSO (upper) and in aqueous media (lower) at three different concentrations: 0.05, 0.1, and 0.2 μM .

3. Summary and conclusions

This study was designed to observe structure–activity relationships of core-modified porphyrins with physico-chemical and biological properties as a continuation of our previous studies.^{5–9} Mono-functionalized dithiaporphyrins 2–5, dihydroxydithiachlorins 6 and 7, and mono-thiaporphyrin 8 with two unsubstituted meso-positions were prepared and compared with dithiaporphyrin 1. Compounds 2–8 were prepared based on our previous methods with slight modification. In the preparation of dihydroxydithiachlorins 6 and 7, OsO_4 was used.¹² Mono-thiaporphyrin 8 was prepared as a surrogate for dithiaporphyrin with only two meso aryl groups.

The photophysical properties were similar within the series of dithiaporphyrins 1–7. The band I absorption maxima of 1–7 were between 694 and 698 nm (665 nm for thiaporphyrin 8). All of the dithiaporphyrins generated singlet oxygen quite effectively and oxidized 62–78% of DPBF (48% for thiaporphyrin 8). The differences observed with 8 might be due to the core system and/or the absence of two meso aryl groups. The unusual

absorption spectrum of dihydroxydithiachlorin 6 relative to tetranitrogenic chlorins was reported.¹² In the tetranitrogenic porphyrins, chlorins usually have longer-wavelength absorption maxima than the corresponding porphyrins. However, chlorins of dithiaporphyrins do not show a similar bathochromic shift. Interestingly, dihydroxydithiachlorins 6 and 7 generated singlet oxygen as effectively as dithiaporphyrin 1. Lipophilicity was affected mainly by the functional groups.

Although none of compounds 2–8 was more potent than 1, we were able to observe relations between structure and activity. The phototoxicity of the core-modified porphyrins was dependent on multiple factors such as intracellular uptake, lipophilicity, the tendency to form aggregates, and singlet-oxygen quantum yield. The higher potency of 6 is attributed to extraordinarily high uptake compared to the other core-modified porphyrin derivatives. The lower efficiency of highly lipophilic porphyrins, for example, 4 and 6, might be, in part, due to the formation of inactive aggregates in the cytoplasm. Water-soluble derivative 7 had the lowest uptake in the series and poor phototoxicity. On the other hand, the poor phototoxicity of 8 might be due to the com-

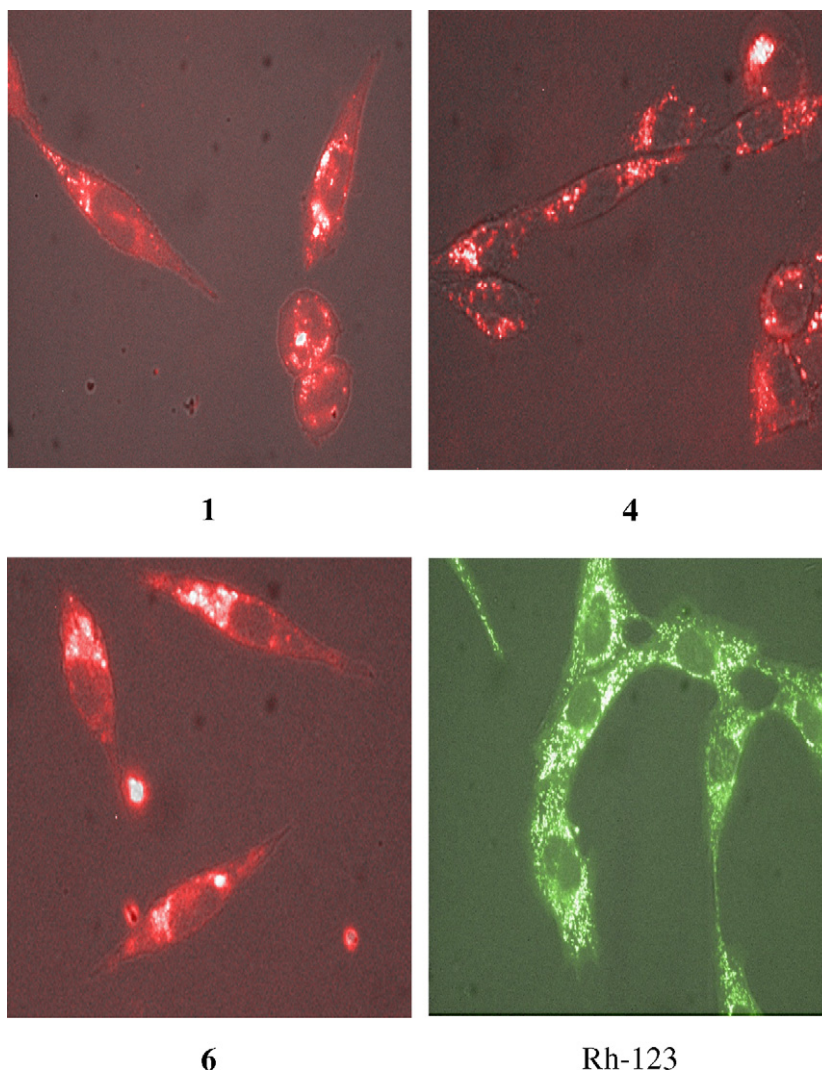


Figure 5. Fluorescence images of R3230AC cells treated with 20 μ M of **1**, **4**, **6**, and 13 μ M of Rh-123. Cell culture conditions and experimental details are described in Section 4.

bined effects of lower uptake and less effective generation of singlet oxygen.

4. Experimental

4.1. General methods

Solvents and reagents were used as received from PHARMCO-AAPER, Sigma-Aldrich Chemical Co. or Thermo Fisher Scientific, Inc. unless otherwise noted. Chemicals for tissue culture were purchased from Sigma-Aldrich Chemical Co. or Thermo Fisher Scientific, Inc. NMR spectra were recorded at 23 $^{\circ}$ C on a Varian Gemini-300, Inova 400 (Bruker AVANCE 400), or Inova 500 instrument with residual solvent signal as the internal standard: CDCl_3 (δ 7.26 for proton, δ 77.16 for carbon). UV–visible near-IR spectra were recorded on a Perkin-Elmer Lambda 12 or CHEM4-UV-FIBER spectrophotometer (Ocean Optics Inc.). Elemental analyses were conducted by Atlantic Microlabs, Inc. Q-TOF 2 electrospray and ESI mass spectrometry were con-

ducted by the Campus Chemical Instrumentation Center of the Ohio State University (Columbus, OH), the Instrument Center of the Department of Chemistry at the University at Buffalo, or the Campus Mass Spectrometry Facility of at South Dakota State University.

4.2. Synthesis

Compounds **1**, **2**, **12**, **16**, **20**, **22**, **23**, and **26** were prepared as previously described in our earlier works.^{5–8,10}

4.2.1. Synthesis of 2-[1-(4-fluorophenyl)-1-hydroxy-methyl]-thiophene (9). Thiophene (12.0 mL, 150 mmol) was added to a solution of *n*-butyllithium (93.8 mL of a 1.6 M solution in hexanes, 150 mmol) and TMEDA (22.7 mL, 150 mmol) in 400 mL of hexanes under an Ar atmosphere. The reaction mixture was heated at reflux for 1 h, cooled to ambient temperature to make 2-lithiophene. This 2-lithiophene suspension was transferred via a cannula to a solution of 4-fluorobenzaldehyde (15.0 mL, 143 mmol) in 400 mL of anhydrous THF cooled to 0 $^{\circ}$ C, which had been degassed with Ar

for 15 min. After the addition was complete, the mixture was warmed to ambient temperature, 500 mL of aqueous 1 M NH_4Cl was added, and the organic phase was separated. The aqueous phase was extracted with ether (3×400 mL). The combined organic extracts were washed with water (3×400 mL) and brine (400 mL), dried over MgSO_4 , and concentrated. The crude product was purified by silica gel column chromatography with the mixture of EtOAc and hexanes giving 13 g (46%) of **9** as a light yellow oil. The structure was confirmed by the comparison with the reference data.²⁷

4.2.2. 2-[1-(4-Fluorophenyl)-1-(tert-butyldimethylsilyloxy)-methyl]thiophene (10). Compound **10** was prepared following literature procedures.⁸ Briefly, a solution of compound **9**, TBSCl (28.0 g, 186 mmol), DMAP (7.5 g, 61 mmol), and Et_3N (11.0 mL, 188 mmol) in 300 mL of dry CH_2Cl_2 was stirred at 0 °C for 2 h and was then warmed to ambient temperature for 24 h. The reaction mixture was partitioned between 400 mL of ether and 400 mL of saturated aqueous NaHCO_3 . The organic layer was washed with water (3×400 mL) and brine (400 mL), dried over MgSO_4 , and concentrated to give a yellow oil. Chromatography on SiO_2 eluted with 25% EtOAc/hexanes gave 14.7 g (74%) of **10** as a colorless oil. ^1H NMR (300 MHz, CDCl_3): δ 0.04 (3H, s), 0.11 (3H, s), 0.99 (9H, s), 6.01 (1H, s), 7.25 (2H, t, $J = 8.7$ Hz), 7.44–7.65 (5H, m); ^{13}C NMR (75 MHz, CDCl_3): δ –4.89, –4.70, 18.42, 25.91, 72.72, 115.10, 115.38, 123.75, 124.86, 126.52, 127.91, 128.02, 140.42, 140.46, 150.33, 160.65, 163.90; HR Q-TOF MS: m/z 345.1105 (calcd for $\text{C}_{17}\text{H}_{23}\text{FOSSi} + \text{Na}$, 345.1121).

4.2.3. 2-[1-(4-Fluorophenyl)-1-hydroxymethyl]-5-[1-(4-methoxyphenyl)-1-hydroxymethyl]thiophene (11). Compound **10** (7.0 g, 22 mmol) was added to a solution of *n*-butyllithium (14.9 mL, 1.6 M in hexanes, 24 mmol) and TMEDA (3.6 mL, 24 mmol) in 50 mL of hexanes under an Ar atmosphere. The reaction mixture was stirred at ambient temperature for 30 min. The suspension of lithio-**10** was transferred dropwise via cannula to a 0 °C solution of 4-methoxybenzaldehyde (2.5 mL, 21 mmol) in anhydrous THF (50 mL), which had been degassed with Ar for 15 min. After addition was complete, the mixture was allowed to warm to ambient temperature, 100 mL of a 1 M solution of NH_4Cl was added, and the organic phase was separated. The aqueous phase was extracted with ether (3×150 mL). The combined organic extracts were washed with water (3×150 mL) and brine (150 mL), dried over MgSO_4 , and concentrated to give a yellow oil. The oil was dissolved in a 1 M solution of Bu_4NF in THF (50 mL, 50 mmol) and stirred at ambient temperature for 1 h at which point 50 mL of saturated aqueous NH_4Cl was added. The resulting mixture was extracted with ether (4×70 mL). The combined organic extracts were washed with water (3×150 mL) and brine (150 mL), dried over MgSO_4 , and concentrated. The crude diol was purified by column chromatography on SiO_2 eluted with 25% EtOAc/hexanes to give 5.5 g (74%) of **11** as a yellow solid. ^1H NMR (400 MHz, CDCl_3): δ 3.73 (3H, s), 5.78 (1H, m), 5.85 (1H, m), 6.02 (1H, d, $J = 3.4$ Hz), 6.17 (1H, d, $J = 3.4$ Hz), 6.65 (2H, m),

6.88 (2H, d, $J = 6.5$ Hz), 7.15 (2H, t, $J = 6.9$ Hz), 7.29 (2H, m), 7.42 (2H, t, $J = 5.2$ Hz); HR Q-TOF MS: m/z 344.0882 (calcd for $\text{C}_{19}\text{H}_{17}\text{FO}_3\text{S}$, 344.0885).

4.2.4. 5,15,20-Tri(4-fluorophenyl)-10-(4-methoxyphenyl)-21,23-dithiaporphyrin (13). Diol **11** (4.0 g, 12 mmol), 2,5-bis[1-(4-fluorophenyl)-1-pyrrolomethyl]thiophene (**12**, 5.0 g, 12 mmol), and 2,3,5,6-tetrachloro-1,4-benzoquinone (TCBQ, 8.6 g, 35 mmol) were dissolved in 500 mL CH_2Cl_2 . *p*-Toluenesulfonic acid monohydrate (2.2 g, 12 mmol) was added and the reaction mixture was stirred for 0.5 h in the dark. The reaction mixture was concentrated and the residue was redissolved in minimal CH_2Cl_2 . The crude product was purified via chromatography on basic alumina eluted with CH_2Cl_2 . A red band containing dithiaporphyrin **13** was isolated. The crude product was washed with acetone to give 0.72 g (9%) of **13** as a purple solid. Mp: >300 °C; ^1H NMR (400 MHz, CDCl_3): δ 4.13 (3H, s), 7.40 (2H, d, $J = 8.6$ Hz), 7.54 (6H, t, $J = 8.6$ Hz), 8.22 (8H, m), 8.68 (3H, m), 8.75 (1H, d, $J = 4.5$ Hz), 9.68 (3H, m) 9.77 (1H, d, $J = 5.0$ Hz); HR ESI MS: m/z 733.1602 (calcd for $\text{C}_{45}\text{H}_{27}\text{F}_3\text{N}_2\text{OS}_2 + \text{H}$, 733.1595).

4.2.5. 5,15,20-Tri(4-fluorophenyl)-10-(4-hydroxyphenyl)-21,23-dithiaporphyrin (14). Dithiaporphyrin **13** (0.47 g, 0.64 mmol) was dissolved in 50 mL of CH_2Cl_2 and BBr_3 (0.2 mL, 1.9 mmol) was added at 0 °C. The resulting solution was stirred overnight at ambient temperature. The reaction mixture was added to 150 mL of EtOAc and 150 mL of saturated NaHCO_3 . The organic layer was separated and washed three times with 150 mL of brine, dried over MgSO_4 , and concentrated. The crude solid was washed with 25% EtOAc/hexanes several times to give 0.38 g (82%) of **14** as a dark blue solid. Mp: >300 °C; ^1H NMR (400 MHz, $\text{DMSO}-d_6$): δ 6.45 (2H, d, $J = 8.5$ Hz), 6.89 (6H, m), 7.23 (2H, d, $J = 8.4$ Hz), 7.45 (6H, m), 7.78 (3H, m), 7.86 (1H, d, $J = 4.5$ Hz), 8.87 (3H, m), 8.97 (1H, d, $J = 5.1$ Hz), 9.26 (1H, s); HR Q-TOF MS: m/z 719.1433 (calcd for $\text{C}_{44}\text{H}_{25}\text{F}_3\text{N}_2\text{OS}_2 + \text{H}$, 719.1442).

4.2.6. 5,15,20-Tri(4-fluorophenyl)-10-[4-(ethoxycarbonylmethyleneoxy)-phenyl]-21,23-dithiaporphyrin (15). Dithiaporphyrin **14** (0.33 g, 0.46 mmol), K_2CO_3 (0.63 g, 4.6 mmol), and ethyl bromoacetate (0.5 mL, 4.6 mmol) in 200 mL acetone were heated at reflux for 10 h. The reaction mixture was cooled to ambient temperature and the K_2CO_3 was removed by filtration. The filter cake was washed with acetone until the filtrate became colorless. The combined filtrates were concentrated. The crude product was washed with MeOH to give 0.32 g (87%) of **15** as a purple solid. Mp: 168–170 °C; ^1H NMR (400 MHz, CDCl_3): δ 1.44 (3H, t, $J = 7.1$ Hz), 4.44 (2H, q, $J = 7.1$ Hz), 4.94 (2H, s), 7.40 (2H, d, $J = 8.6$ Hz), 7.54 (6H, t, $J = 8.6$ Hz), 8.22 (8H, m), 8.68 (3H, m), 8.73 (1H, d, $J = 4.5$ Hz), 9.67 (3H, m), 9.74 (1H, d, $J = 5.1$ Hz); HR Q-TOF MS: m/z 805.1801 (calcd for $\text{C}_{48}\text{H}_{31}\text{F}_3\text{N}_2\text{O}_3\text{S}_2 + \text{H}$, 805.1812).

4.2.7. 5,15,20-Tri(4-fluorophenyl)-10-[4-(carboxymethyleneoxy)-phenyl]-21,23-dithiaporphyrin (3). Core-modified porphyrin **15** (0.30 g, 0.37 mmol) was dissolved in

40 mL THF and 40 mL of 1 M aqueous NaOH was added. The resulting solution was stirred at ambient temperature for 15 h. The solution was acidified by the addition of 4.1 mL of 10 N HCl. The reaction mixture was diluted with 100 mL H₂O and the products were extracted with EtOAc (3 × 100 mL). The combined organic extracts were dried over MgSO₄ and concentrated. The crude product was washed with several portions of hexanes/MeOH to give 0.19 g (66%) of **3** as a purple solid. Mp: >300 °C; ¹H NMR (400 MHz, DMSO-*d*₆): δ 4.15 (2H, s), 6.59 (2H, d, *J* = 8.6 Hz), 6.88 (6H, t, *J* = 8.7 Hz), 7.34 (2H, d, *J* = 8.6 Hz), 7.44 (6H, m), 7.78 (3H, m), 7.82 (1H, d, *J* = 4.5 Hz), 8.88 (3H, m), 8.93 (1H, d, *J* = 5.1 Hz); HR Q-TOF MS: *m/z* 777.1509 (calcd for C₄₆H₂₇F₃N₂O₃S₂ + H, 777.1488).

4.2.8. 5-(4-*tert*-Butylphenyl)-10-(4-methoxyphenyl)-15,20-bis-phenyl-21,23-dithiaporphyrin (16). Dithiaporphyrin **16** was prepared as previously described.¹⁰

4.2.9. 5-(4-*tert*-Butylphenyl)-10-(4-hydroxyphenyl)-15,20-diphenyl-21,23-dithiaporphyrin (17). Dithiaporphyrin **17** (0.16 g, 0.21 mmol) was treated with BBr₃ (0.25 mL, 2.7 mmol) as described for the preparation of **14** to give 0.14 g (92%) of **17** as a metallic purple solid. Mp: >300 °C; ¹H NMR (500 MHz, CDCl₃): δ 9.71 (4H, dd, *J* = 4.9, 8.8 Hz), 8.71 (4H, dd, *J* = 4.3, 6.1 Hz), 8.25 (4H, dd, *J* = 1.6 Hz, 5.5 Hz), 8.19 (2H, d, *J* = 7.9 Hz), 8.11 (2H, d, *J* = 8.2 Hz), 7.82 (8H, dd, *J* = 7.9 Hz, 8.2 Hz), 7.23 (2H, d, *J* = 8.5 Hz), 5.09 (1H, br s), 1.62 (9H, s); ¹³C NMR (300 MHz, CDCl₃): δ 157.2, 156.6, 151.5, 148.5, 148.3, 141.8, 138.7, 136.1, 135.8, 135.2, 134.9, 134.9, 134.8, 134.7, 134.7, 134.4, 134.3, 128.5, 127.9, 125.0, 115.0, 35.5, 32.2; HR ESI MS: *m/z* 721.2693 (calcd for C₄₈H₃₆ON₂S₂ + H, 721.2710).

4.2.10. 5-(4-*tert*-Butylphenyl)-10-[4-(ethoxycarbonylmethyleneoxy)-phenyl]-15,20-bis-phenyl-21,23-dithiaporphyrin (18). Dithiaporphyrin **17** (0.14 g, 0.19 mmol) was reacted with ethyl bromoacetate (0.67 mL, 6.0 mmol) and K₂CO₃ (0.82 g, 5.8 mmol) in 50 mL of acetone as described for the preparation of **15** to give 0.15 g (95%) of **18** as a dark purple solid. Mp: 185–187 °C; ¹H NMR (500 MHz, CDCl₃): δ 9.70 (4H, dd, *J* = 4.9, 8.8 Hz), 8.70 (4H, dd, *J* = 4.0, 6.1 Hz), 8.22 (8H, dd, *J* = 5.8, 8.2 Hz), 7.82 (8H, dd, *J* = 7.3, 8.8 Hz), 7.36 (2H, d, *J* = 7.3 Hz), 4.92 (2H, s), 4.42 (2H, q, *J* = 7.0 Hz), 1.61 (9H, s), 1.42 (3H, t, *J* = 7.2 Hz); ¹³C NMR (300 MHz, CDCl₃): δ 169.5, 158.6, 157.2, 156.9, 151.5, 148.4, 148.4, 141.9, 138.8, 136.2, 135.9, 135.3, 135.0, 134.9, 134.8, 134.5, 134.4, 134.1, 134.0, 128.5, 128.0, 125.0, 114.3, 66.3, 62.1, 35.5, 32.2, 14.8; HR ESI MS: *m/z* 807.2693 (calcd for C₅₂H₄₃O₃N₂S₂ + H, 807.2710).

4.2.11. 5-(4-*tert*-Butylphenyl)-10-[4-(carboxymethyleneoxy)-phenyl]-15,20-bis-phenyl-21,23-dithiaporphyrin (4). Dithiaporphyrin **18** (0.15 g, 0.18 mmol) was hydrolyzed by 1 M NaOH (16 mL) as described for the preparation of **3** to give 0.095 g (68%) of **4** as a purple solid; mp: >300 °C. ¹H NMR (500 MHz, CDCl₃): δ 9.69 (4H, dd, *J* = 4.9, 8.8 Hz), 8.67 (4H, dd, *J* = 4.3, 7.9 Hz), 8.17

(8H, m), 7.81 (8H, dd, *J* = 5.2, 8.2 Hz), 7.35 (2H, dd, *J* = 7.6 Hz), 4.94 (2H, s), 1.62 (9H, s); ¹³C NMR (300 MHz, CDCl₃): δ 158.2, 157.1, 156.8, 151.5, 148.5, 148.3, 141.7, 138.7, 136.1, 135.9, 135.5, 135.2, 134.9, 134.9, 134.7, 134.5, 134.4, 133.7, 128.6, 127.9, 125.0, 114.3, 65.7, 35.5, 32.2; HR ESI MS: *m/z* 779.2421 (calcd for C₅₀H₃₉O₃N₂S₂ + H, 779.2397).

4.2.12. 2-[1-(4-Fluorophenyl)-1-pyrrolomethyl]-5-[1-phenyl-1-pyrrolomethyl]-thiophene (19). 2-[1-(4-Fluorophenyl)-1-hydroxymethyl]-5-[1-phenyl-1-hydroxymethyl]-thiophene⁵ (6.0 g, 18 mmol) was dissolved in excess pyrrole (25 mL). Boron trifluoride etherate was added (0.40 mL, 3.6 mmol) and the resulting mixture was stirred for 1 h at ambient temperature. The reaction was stopped by the addition of CH₂Cl₂ (150 mL), followed by 40% NaOH (80 mL). The organic layer was separated, washed with water (3 × 200 mL) and brine (200 mL), dried over MgSO₄, and concentrated. The excess pyrrole was removed at reduced pressure at ambient temperature. The residual oil was purified via chromatography on SiO₂ eluted with 25% EtOAc/hexanes to give 5.0 g (68%) of **19** as a yellow oil. ¹H NMR (400 MHz, CDCl₃): δ 5.61 (1H, s), 5.63 (1H, s), 5.96 (1H, s), 6.00 (1H, s), 6.22 (2H, s), 6.67 (1H, s), 6.69 (1H, s), 6.76 (2H, s), 7.06 (2H, dd, *J* = 8.1, 7.9 Hz), 7.23–7.36 (5H, m), 7.38 (2H, d, *J* = 6.8 Hz), 7.95 (2H, br s); HR EI MS: *m/z* 412.1404 (calcd for C₂₆H₂₁FN₂S, 412.1404).

4.2.13. 5,15,20-Tri-(4-fluorophenyl)-10-phenyl-21,23-dithiaporphyrin (21). Cyclization of 2,5-bis[(4-fluorophenyl)-hydroxymethyl]-thiophene⁷ (**20**, 2.9 g, 7.0 mmol) and **19** (2.3 g, 6.9 mmol) with TsOH·H₂O (1.3 g, 6.9 mmol) and TCBQ (5.1 g, 21 mmol) was performed as described for the preparation of **13** to give 0.67 g (14%) of **21** as a purple solid; mp: >300 °C. ¹H NMR (400 MHz, CDCl₃): δ 7.55 (6H, m), 7.85 (3H, m), 8.23 (8H, m), 8.69 (4H, m), 9.68 (4H, m); HR EI MS: *m/z* 702.1406 (calcd for C₄₄H₂₅F₃N₂S₂, 702.1407).

4.2.14. 5,15,20-Tri-(4-fluorophenyl)-10-(4-sulfonatophenyl)-21,23-dithiaporphyrin sodium salt (5). Dithiaporphyrin **21** (0.30 g, 0.43 mmol) was dissolved in excess concentrated H₂SO₄ (40 mL) and allowed to stir at 100 °C overnight. The acid was slowly neutralized with concentrated NaOH until the solution was slightly basic. An equal volume of MeOH was added, and the solid Na₂SO₄ was removed by filtration. The filtrate was concentrated, and the residue was dissolved in acetone. The resulting solution was chilled precipitating more Na₂SO₄, which was removed via filtration. The acetone solution was concentrated, and the residue was recrystallized from 10% aqueous MeOH to give 0.17 g (50%) of **5** as a purple solid. Mp: >300 °C; ¹H NMR (400 MHz, CD₃OD): δ 7.78 (6H, t, *J* = 8.4 Hz), 8.16 (2H, d, *J* = 7.3 Hz), 8.26 (2H, d, *J* = 7.4 Hz), 8.35 (6H, t, *J* = 5.8 Hz), 8.67–8.73 (4H, s), 9.76–9.83 (4H, s); HR ESI MS: *m/z* 783.1052 (calcd for C₄₄H₂₄F₃N₂O₃S₃ + H, 783.1069).

4.2.15. 5,20-Bis-phenyl-10,15-bis[4-(ethoxycarbonylmethyleneoxy)-phenyl]-21,23-dithia-7,8-dihydroxychlorin (24). Dihydroxylation of dithiaporphyrin **23** followed litera-

ture procedures.¹² Briefly, dithiaporphyrin **23** (0.60 g, 0.70 mmol) was dissolved in a 100:1 mixture of CHCl_3 :pyridine (140 mL). To the solution, OsO_4 (0.27 g, 1.1 mmol) was added and the flask was closed with stoppers, covered with aluminum foil, and stirred at ambient temperature for 3 d. The reaction was then quenched by purging with H_2S for 5 min and the excess H_2S was trapped by 6 M NaOH aqueous solution. The solution was filtered through a plug of Celite and the filtrate was evaporated. The resulting residue was purified on a silica gel column eluted with a mixture of CH_2Cl_2 and MeOH to give 0.15 g (24%) of **24** as a purple solid. ^1H NMR (400 MHz, $\text{CDCl}_3 + \text{CD}_3\text{OD}$): δ 1.39 (3H, t, $J = 4.4$ Hz), 1.42 (3H, t, $J = 4.7$ Hz), 3.19 (1H, d, $J = 4.2$ Hz), 3.25 (1H, d, $J = 4.3$ Hz), 4.35–4.44 (4H, s), 4.87 (2H, s), 4.90 (2H, s), 6.38–6.47 (2H, m), 7.19 (4H, s), 7.28–7.35 (2H, m), 7.70–7.83 (5H, m), 7.80 (1H, d, $J = 7.9$ Hz), 7.92–7.98 (1H, m), 8.04–8.24 (5H, m), 8.46–8.54 (2H, m), 9.12 (2H, t, $J = 7.1$ Hz), 9.45 (1H, d, $J = 5.0$ Hz), 9.48 (1H, d, $J = 4.9$ Hz); HR ESI MS: m/z 887.2974 (calcd for $\text{C}_{52}\text{H}_{42}\text{N}_2\text{O}_8\text{S}_2 + \text{H}$, 887.2461).

4.2.16. 5,20-Diphenyl-10,15-bis[4-(carboxymethyleneoxy)-phenyl]-21,23-dithia-7,8-dihydroxychlorin (7). Dithiaporphyrin **24** (0.14 g, 0.16 mmol) was hydrolyzed by 1 M NaOH (40 mL) as described for the preparation of **3** to give 0.10 g (76%) of **7** as a purple solid. ^1H NMR (400 MHz, $\text{CDCl}_3 + \text{CD}_3\text{OD}$): δ 4.87 (2H, s), 4.90 (2H, s), 6.36 (2H, s), 7.29 (1H, dd, $J = 6.1$, 1.8 Hz), 7.30–7.40 (3H, m), 7.59 (2H, s), 7.65–7.93 (7H, m), 8.03–8.24 (5H, m), 8.39 (1H, d, $J = 4.4$ Hz), 8.42 (1H, d, $J = 4.4$ Hz), 9.13 (1H, d, $J = 5.0$ Hz), 9.17 (1H, d, $J = 5.0$ Hz), 9.47 (1H, d, $J = 5.0$ Hz), 9.51 (1H, d, $J = 5.0$ Hz); HR ESI MS: m/z 831.2313 (calcd for $\text{C}_{48}\text{H}_{34}\text{N}_2\text{O}_8\text{S}_2 + \text{H}$, 831.1835).

4.2.17. 5,20-Bis-phenyl-12,13-dimethoxy-21-thiaporphyrin (27). Cyclization of 2,5-bis(hydroxymethyl)-3,4-dimethoxy-thiophene²⁸ **25** (0.50 g, 2.5 mmol), pyrrole (0.52 mL, 7.5 mmol), and benzaldehyde (0.42 mL, 4.2 mmol) with BF_3 :etherate (0.052 mL, 0.41 mmol) and TCBQ (1.7 g, 7.4 mmol) was performed as described for the preparation of **13** to give 0.08 g (6%) of **27** as a purple solid. Mp: 159–161 °C; ^1H NMR (500 MHz, CDCl_3): δ 4.73 (6H, s), 7.60–7.72 (6H, m), 8.06 (4H, d, $J = 5.4$ Hz), 8.56 (2H, d, $J = 3.5$ Hz), 8.71 (2H, s), 8.89 (2H, d, $J = 3.5$ Hz), 10.42 (2H, s); HR ESI MS: m/z 540.2460 (calcd for $\text{C}_{34}\text{H}_{25}\text{N}_3\text{O}_2\text{S} + \text{H}$, 540.1746).

4.2.18. 5,20-Bis-phenyl-12,13-dihydroxy-21-thiaporphyrin (28). Mono-thiaporphyrin **27** (0.18 g, 0.33 mmol) was demethylated with BBr_3 (0.16 mL, 1.67 mmol) in CH_2Cl_2 as described for the preparation of **14** to give 0.15 g (88%). The crude product was used without further purification.

4.2.19. 5,20-Bis-phenyl-12,13-bis(ethoxycarbonylmethylenoxy)-21-thiaporphyrin (29). Mono-thiaporphyrin **28** (0.30 g, 0.59 mmol) was treated with ethyl bromoacetate (0.70 mL, 5.9 mmol) and K_2CO_3 (0.81 g, 5.9 mmol) in 150 mL of acetone as described for the preparation of **15** to give 0.20 g (51%) of **29** as a dark purple solid.

Mp: 119–121 °C; ^1H NMR (400 MHz, CDCl_3): δ 1.38 (6H, t, $J = 7.1$ Hz), 4.44 (4H, q, $J = 7.1$ Hz), 5.76 (4H, s), 7.75 (9H, m), 8.18 (4H, d, $J = 7.9$ Hz), 8.67 (2H, d, $J = 4.4$ Hz), 8.91 (1H, d, $J = 1.9$ Hz), 9.01 (2H, d, $J = 4.4$ Hz), 10.71 (1H, s); HR ESI MS: m/z 684.2468 (calcd for $\text{C}_{40}\text{H}_{33}\text{N}_3\text{O}_6\text{S} + \text{H}$, 684.2168).

4.2.20. 5,20-Bis-phenyl-12,13-carboxylatomethoxy-21-thiaporphyrin (8). Mono-thiaporphyrin **30** (0.20 g, 0.29 mmol) was hydrolyzed by 1 M NaOH (4 mL) as described for the preparation of **3** to give 0.10 g (55%) of **8** as a purple solid. Mp: 199–201 °C; ^1H NMR (400 MHz, CDCl_3): δ -1.61 (1H, br s), 7.86 (4H, s), 8.22 (6H, s), 8.22 (4H, s), 8.56 (2H, s), 8.92 (2H, s), 8.92 (2H, s), 10.82 (2H, s), 12.12 (2H, s); HR ESI MS: m/z 628.1807 (calcd for $\text{C}_{36}\text{H}_{25}\text{N}_3\text{O}_6\text{S} + \text{H}$, 628.1542).

4.3. Photophysical properties

4.3.1. Relative quantum yields for singlet oxygen generation. A stock solution of 1,3-diphenylisobenzofuran (DPBF) (A, 180 μM) was prepared by dissolving 4.9 mg of DPBF in 100 mL of THF. Stock solutions of the porphyrins (B, 2 mM) were prepared by dissolving the desired amount of porphyrin in THF. Ten microliters of (B) was added to 10 mL of THF to get a 2 μM stock solution of the porphyrins (C). The reaction mixture was prepared by mixing 2 mL of (A) and 2 mL of (C), so that the final concentration of DPBF is 90 μM and that of porphyrin is 1 μM .

The UV absorbance of the reaction mixture was obtained before irradiation, using THF as a blank solution. The irradiation was carried out using a halogen lamp with a water filter (400–850 nm). The light intensity was 3 mW/cm^2 and the reaction mixture was continuously stirred during the irradiation. The progress of reaction was monitored after every 2 min of irradiation up to 10 min, using UV absorbance. 300 μL of the sample was used each time for UV measurement.

4.3.2. Determination of *n*-octanol/water partition coefficients at pH 7.4 phosphate buffer. The *n*-octanol/water partition coefficients were determined at pH 7.4 using the absorbance of the core-modified porphyrins. A 'shake flask' direct measurement²⁹ with minor modification was used. Individual porphyrins were dissolved in a mixture of equal volumes of *n*-octanol and a pH 7.4 phosphate buffer, then placed in an ultrasound bath for 30 min. The mixture was then left to settle for 4 h and the partition coefficients determined by measuring the absorbance of the core-modified porphyrins, using an Ocean Optics USB4000 UV–vis spectrometer. Results were reported as $\log D_{7.4}$ values.

4.4. Biology

4.4.1. Cells and culture conditions. Cells cultured from the rodent mammary adenocarcinoma cell line (R3230AC) were used. The cells were maintained on 60 mm diameter polystyrene dishes (Becton Dickinson Labware, Franklin lakes, NJ) in 7 mL minimum essential medium (α -MEM) supplemented with 10% bovine

growth serum (HyClone, No.: SH3054103), 50 units/mL penicillin G, 50 µg/mL streptomycin, and 1.0 g/mL fungizone (complete medium). Cells were incubated at 37 °C in 5% CO₂ using an incubator (Sanyo MCO-18AIC-UV). Passage was accomplished by aspirating the culture medium, then adding a 1.0 mL solution containing 0.25% trypsin and waiting for 4–5 min to remove the cells from the dish's surface. New culture dishes were then seeded with the appropriate number of cells in 7.0 mL of complete medium. Cell counts were done using a hemacytometer. The cell doubling time was approximately 20 h.

4.4.2. Incubation of cell cultures with dithiaporphyrins. In experiments to determine the porphyrin intracellular accumulation, R3230AC cells were seeded on 96-well plates at cell densities between 2.0 and 3.0 × 10⁴ cells/well in the complete medium and incubated at 37 °C in 5% CO₂ for 24 h. The porphyrins were dissolved in DMSO at 2 mM. The stock solutions were diluted to the appropriate concentrations with complete medium immediately before the addition to cells. The porphyrin samples were then added to the wells and incubated for 24 h. After incubation, the medium was removed and the cell monolayer rinsed twice with a 0.9% NaCl solution. 190 µL of DMSO was then added to solubilize the cells and the fluorescence from the porphyrins read using a fluorescence multi-well plate reader (Molecular Devices, SpectraMax M2 model) set at the appropriate excitation and emission wavelengths. The intracellular porphyrin concentrations were then determined from a standard fluorescence curve obtained by dissolving porphyrin standards in DMSO. Results were expressed in fmol/cell.

In experiments to determine the cytotoxicity of the porphyrins in either the dark (dark toxicity) or after light exposure (phototoxicity), R3230AC cells were seeded on 96-well plates at cell densities between 1.0 and 1.5 × 10⁴ cells/well in the complete medium. Cultures were then incubated for 24 h at 37 °C in 5% CO₂, and then the porphyrins, dissolved in the complete medium to the appropriate concentrations, were added to the wells and again incubated for 24 h. The medium was then removed and the cell monolayer rinsed twice with 190 µL of a 0.9% NaCl solution. Clear medium without phenol red and bovine growth serum, was then added to the wells and the well plates either kept in the dark (dark toxicity) or irradiated (phototoxicity) for an hour. After this the clear medium was removed and 190 µL of complete medium added. The cultures were then incubated at 37 °C in 5% CO₂, for 24 h, after which the cytotoxicity was determined by MTT assay and expressed as a percent of the controls. The controls used in the dark toxicity tests were cells kept in the dark and in the absence of porphyrins, while those used in the phototoxicity tests were cells exposed to light in the absence of porphyrins.

4.4.3. Irradiation of cultured cells. After 24 h of incubation with the porphyrins, the medium was removed, and the cell monolayer was rinsed twice with 190 µL of a 0.9% NaCl solution. Clear medium, was then added to the wells and the well plate placed on an orbital sha-

ker (Lab-line, Barnstead International, IA). The well plate's lid was then removed and the wells exposed for an hour to broadband visible light delivered at 3 mW cm⁻² from a 60 W halogen light source, through a 3.5 cm water filter (400–850 nm). Uniform illumination of the entire well plate was achieved by gently orbiting the well plate on the shaker. After an hour of irradiation, the clear medium was removed, and 190 µL of complete medium added to the wells. The cultures were incubated at 37 °C in 5% CO₂, and in the dark for 24 h, after which the cytotoxicity was determined by MTT assay and expressed as a percent of the controls, cells exposed to light in the absence of porphyrins.

4.4.4. Fluorescence microscopy with thiaporphyrins. R3230AC cells were seeded at cell densities between 2.0 and 3.0 × 10⁴ cells/well in a 24-well plate containing 12 mm diameter coverslips in 1 mL of complete medium and then incubated at 37 °C in 5% CO₂ for 24 h. The porphyrin samples, dissolved in medium, were then added to the well plate at 2.0 × 10⁻⁵ M and incubated again for 24 h. The medium was then removed and the cell monolayer rinsed twice with 3 mL of complete medium. After this the cover slide was immediately removed and mounted on a slide and the images taken. The images were captured using a Leica DMI4000B fluorescence microscope fitted with a QImaging Fast 1394 camera and Qcapture processing software. The images were modified for better visualization with Adobe Photoshop Element 5.0.

4.4.5. Statistical analyses. Statistical analyses were performed using the Student's *t*-test for pairwise comparisons. A *P* value of <0.05 was considered significant. The Hill (sigmoid Emax) equation was fitted to the data to obtain IC₅₀ values.

Acknowledgments

This research was supported by the Department of Defense [Breast Cancer Research Program] under award number (W81XWH-04-1-0500). Views and opinions of, and endorsements by, the author(s) do not reflect those of the US Army or the Department of Defense.

References and notes

1. Dougherty, T. J.; Gomer, C. J.; Henderson, B. W.; Jori, G.; Kessel, D.; Korbek, M.; Moan, J.; Peng, Q. *J. Natl. Cancer Inst.* **1998**, *90*, 889.
2. Dolmans, D. E.; Fukumura, D.; Jain, R. K. *Nat. Rev. Cancer* **2003**, *3*, 380.
3. Sternberg, E. D.; Dolphin, D.; Bruckner, C. *Tetrahedron* **1998**, *54*, 4151.
4. Detty, M. R.; Gibson, S. L.; Wagner, S. J. *J. Med. Chem.* **2004**, *47*, 3897.
5. You, Y.; Gibson, S. L.; Detty, M. R. *Bioorg. Med. Chem.* **2005**, *13*, 5968.
6. Stilts, C. E.; Nelen, M. I.; Hilme, D. G.; Davies, S. R.; Gollnick, S. O.; Oseroff, A. R.; Gibson, S. L.; Hilf, R.; Detty, M. R. *J. Med. Chem.* **2000**, *43*, 2403.

7. Hilmeý, D. G.; Abe, M.; Nelen, M. I.; Stilts, C. E.; Baker, G. A.; Baker, S. N.; Bright, F. V.; Davies, S. R.; Gollnick, S. O.; Oseroff, A. R.; Gibson, S. L.; Hilf, R.; Detty, M. R. *J. Med. Chem.* **2002**, *45*, 449.
8. You, Y.; Gibson, S. L.; Hilf, R.; Davies, S. R.; Oseroff, A. R.; Roy, I.; Ohulchanskyy, T. Y.; Bergey, E. J.; Detty, M. R. *J. Med. Chem.* **2003**, *46*, 3734.
9. You, Y.; Gibson, S. L.; Hilf, R.; Ohulchanskyy, T. Y.; Detty, M. R. *Bioorg. Med. Chem.* **2005**, *13*, 2235.
10. You, Y.; Daniels, T. S.; Dominiak, P. M.; Detty, M. R. *J. Porphyrins Phthalocyanines* **2007**, *11*, 1.
11. You, Y.; Gibson, S. L.; Detty, M. R. *J. Photochem. Photobiol., B* **2006**, *85*, 155.
12. Lara, K. K.; Rinaldo, C. R.; Bruckner, C. *Tetrahedron Lett.* **2003**, *44*, 7793.
13. Tong, T.-H.; Chien, L.-C. *J. Polym. Sci., A: Polym. Chem.* **2000**, *38*, 1450.
14. Latos-Grazynski, L. In *The Porphyrin Handbook*; Kadish, L. M., Smith, K. M., Guillard, R., Eds.; Academic Press: San Diego, 2000; Vol. 2, p 391.
15. Krieg, M. J. *Biochem. Biophys. Methods* **1993**, *27*, 143.
16. Mosmann, T. *J. Immunol. Methods* **1983**, *65*, 55.
17. Akins, D. L.; Ozcelik, S.; Zhu, H. R.; Guo, C. *J. Phys. Chem.* **1996**, *100*, 14390.
18. Kano, K.; Minamizono, H.; Kitae, T.; Negi, S. *J. Phys. Chem. A* **1997**, *101*, 6118.
19. Juzeniene, A.; Moan, J. *Photodiagn. Photodyn. Ther.* **2007**, *4*, 3.
20. Moan, J. J. *Photochem. Photobiol. B* **1990**, *6*, 343.
21. Kamat, J. P.; Devasagayam, T. P. *Toxicology* **2000**, *155*, 73.
22. Ichinose, S.; Usuda, J.; Hirata, T.; Inoue, T.; Ohtani, K.; Maehara, S.; Kubota, M.; Imai, K.; Tsunoda, Y.; Kuroiwa, Y.; Yamada, K.; Tsutsui, H.; Furukawa, K.; Okunaka, T.; Oleinick, N. L.; Kato, H. *Int. J. Oncol.* **2006**, *29*, 349.
23. Chernyak, B. V.; Izyumov, D. S.; Lyamzaev, K. G.; Pashkovskaya, A. A.; Pletjushkina, O. Y.; Antonenko, Y. N.; Sakharov, D. V.; Wirtz, K. W.; Skulachev, V. P. *Biochim. Biophys. Acta* **2006**, *1757*, 525.
24. Morgan, J.; Oseroff, A. R. *Adv. Drug Deliv. Rev.* **2001**, *49*, 71.
25. Hilf, R. *J. Bioenerg. Biomembr.* **2007**, *39*, 85.
26. Johnson, L. V.; Walsh, M. L.; Chen, L. B. *Proc. Natl. Acad. Sci. U.S.A.* **1980**, *77*, 990.
27. Stoner, E. J.; Cothron, D. A.; Balmer, M. K.; Roden, B. A. *Tetrahedron* **1995**, *51*, 11043.
28. Agarwal, N.; Hung, C. H.; Ravikanth, M. *Eur. J. Org. Chem.* **2003**, *2003*, 3730.
29. Sangster, J. *Octanol–Water Partition Coefficients*; Wiley: New York, 1997.

Dithiaporphyrin Derivatives as Photosensitizers in Membranes and Cells

Rafael Minnes,[†] Hana Weitman,[†] Youngjae You,[‡] Michael R. Detty,^{*,‡} and Benjamin Ehrenberg^{*,†,#}*Department of Physics and Nano Medicine Research Center, Institute of Nanotechnology and Advanced Materials, Bar Ilan University, Ramat Gan 52900, Israel, and Department of Chemistry, University at Buffalo, The State University of New York, Buffalo, New York 14260**Received: August 27, 2007; In Final Form: December 23, 2007*

We synthesized a series of analogues of 5,20-diphenyl-10,15-bis(4-carboxylatomethoxy)phenyl-21,23-dithiaporphyrin (**I**) as potential photosensitizers for photodynamic therapy (PDT). The photosensitizers differ in the length of the side chains that bind the carboxyl to the phenol at positions 10 and 15 of the thiaporphyrin. The spectroscopic, photophysical, and biophysical properties of these photosensitizers are reported. The structural changes have almost no effect on the excitation/emission spectra with respect to **I**'s spectra or on singlet oxygen generation in MeOH. All of the photosensitizers have a very high, close to 1.00, singlet oxygen quantum yield in MeOH. On the contrary, singlet oxygen generation in liposomes was considerably affected by the structural change in the photosensitizers. The photosensitizers possessing short side chains (one and three carbons) showed high quantum yields of around 0.7, whereas the photosensitizers possessing longer side chains showed smaller quantum yield, down to 0.14 for compound **X** (possessing side-chain length of 10 carbons), all at 1 μ M. Moreover a self-quenching process of singlet oxygen was observed, and the quantum yield decreased as the photosensitizer's concentration increased. We measured the binding constant of **I** to liposomes and found $K_b = 23.3 \pm 1.6$ (mg/mL)⁻¹. All the other photosensitizers with longer side chains exhibited very slow binding to liposomes, which prevented us from assessing their K_b 's. We carried out fluorescence resonance energy transfer (FRET) measurements to determine the relative depth in which each photosensitizer is intercalated in the liposome bilayer. We found that the longer the side chain the deeper the photosensitizer core is embedded in the bilayer. This finding suggests that the photosensitizers are bound to the bilayer with their acid ends close to the aqueous medium interface and their core inside the bilayer. We performed PDT with the dithiaporphyrins on U937 cells and R3230AC cells. We found that the dark toxicity of the photosensitizers with the longer side chain (**X**, **VI**, **V**) is significantly higher than the dark toxicity of sensitizers with shorter side chains (**I**, **III**, **IV**). Phototoxicity measurements showed the opposite direction; the photosensitizers with shorter side chains were found to be more phototoxic than those with longer side chains. These differences are attributed to the relationship between diffusion and endocytosis in each photosensitizer, which determines the location of the photosensitizer in the cell and hence its phototoxicity.

Introduction

Photodynamic therapy (PDT) has considerable potential as a treatment of various diseases involving cell hyperproliferation and especially cancer.^{1–5} PDT involves delivery of the photosensitizer to the site of biological action followed by activation by light of an appropriate wavelength. As a result of the illumination, reactive species such as singlet oxygen are produced. Singlet oxygen interacts with biomolecules to damage cellular organelles, which leads to cellular death and tumor degeneration.^{6,7} The search for better, more efficient, photosensitizers for PDT has attracted the attention of researchers in the field. Two desirable properties of photosensitizers that are of major interest for optimal usage are (1) good uptake by cells with preferential, or selective, uptake by cancerous tissues and (2) high quantum yield of singlet oxygen generation.^{1,8}

The advantages of 21,23-dithiaporphyrins (Figure 1) as photosensitizers were established in previous works.^{9–11} The substitution of a S atom for NH groups at the 21 and 23 positions gave a red shift of the absorption maxima,^{8,12,13} which allows wavelengths of light with greater penetration in tissue to be used for PDT treatments. In addition, the core modification also endows 21,23-dithiaporphyrins with a very high efficiency of singlet oxygen generation.^{14,15} In vitro studies have shown that 21,23-dithiaporphyrins have greater phototoxicity when compared to natural porphyrins or 21,23-diselenaporphyrins.⁹

Previous studies indicated that the dicarboxylic acid compound, 5,20-diphenyl-10,15-bis(4-carboxylatomethoxy)phenyl-21,23-dithiaporphyrin (**I**) (Figure 1), is more promising as a photosensitizer than most of the 21,23-dithiaporphyrin derivatives tested. Compound **I** showed high tumor selectivity, low dark toxicity, and high phototoxicity.

We have synthesized a series of new photosensitizers, derivatives of 21,23-dithiaporphyrin, with small alterations from the basic structure of **I**. The photosensitizers differ in the length of the side chains that bind the carboxyl group to the phenol at positions 10 and 15 of the dithiaporphyrin (Figure 1). Molecules

* To whom correspondence should be addressed. Tel.: +972-3-5318427 (B.E.); (716) 645-6800 (M.R.D.). Fax: +972-3-7384054 (B.E.); (716) 645-6963 (M.R.D.). E-mail: ehren@mail.biu.ac.il (B.E.); mdetty@buffalo.edu (M.R.D.).

[†] Bar Ilan University.

[‡] The State University of New York.

[#] Incumbent of the Falk Chair in Laser Phototherapy.

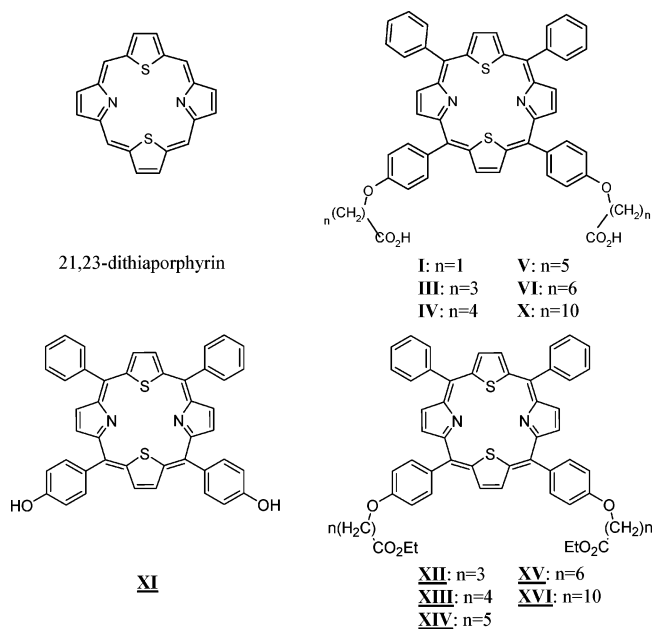


Figure 1. Molecular structures of the 21,23-dithiaporphyrin derivatives and intermediates in their preparation. The photosensitizers have the basic structure of 5,10,15,20-tetraaryl-21,23-dithiaporphyrin. They differ in the length of the side chain that binds the carboxyl to the phenol at positions 10 and 15 of the dithiaporphyrin.

with side-chain lengths of 1 (**I**), 3 (**III**), 4 (**IV**), 5 (**V**), 6 (**VI**), and 10 (**X**) carbons were prepared. We found in this study that these structural changes have a small effect on the photophysical properties of the photosensitizers in solution. The absorption and emission spectra and the quantum yield of the generation of singlet oxygen in MeOH of all the new photosensitizers are very similar to those of **I**. However, a significant effect on the quantum yield of the generation of singlet oxygen in liposomes is shown in the current study. Although most of the photophysical properties are similar in this series, biological properties such as dark toxicity, phototoxicity, and cellular uptake vary for each molecule.

Materials and Methods

Chemicals and Sample Preparation. Solvents and reagents were obtained from Sigma-Aldrich Chemical (St. Louis, MO) unless otherwise noted. L- α -Phosphatidylcholine (PC, L- α -lecithin) type XIII-E from egg yolk (99%, 100 mg/mL ethanol) was a mixture of lipids with the following fatty acid makeup: 33% palmitic (C16:0), 31% oleic (C18:1), 13% stearic (C18:0), and 15% linoleic (C18:2). The remaining 8% is a mixture of several other fatty acids (Sigma Chemical, personal communication). *N*-(5-Dimethylaminonaphthalene-1-sulfonyl)-1,2-dihexadecanoyl-*sn*-glycero-3-phosphoethanolamine, triethylammonium salt (dansyl-DHPE) was obtained from Molecular Probes (Eugene, OR). Diethyl ether (>99.8%) was obtained from Fluka Chemie (Buchs, Switzerland). Dimethyl sulfoxide (DMSO) was obtained from Merck (Darmstadt, Germany). Methanol was obtained from Frutarom Ltd. (Haifa, Israel). Dimethylformamide (DMF) was obtained from Bio-Lab Ltd. (Jerusalem, Israel). Solvents and reagents were used as received unless otherwise noted.

Concentration in vacuo was performed on a Büchi rotary evaporator. NMR spectra were recorded at 23 °C on a Bruker 400 instrument with residual solvent signal as the internal standard: CDCl₃ (δ 7.26 for proton, δ 77.36 for carbon) or CD₃OD (δ 50.41 for carbon). Elemental analyses were con-

ducted by Atlantic Microlabs, Inc. (Norcross, GA). Q-TOF 2 electrospray and ESI mass spectrometry were conducted at the Campus Chemical Instrumentation Center of The Ohio State University (Columbus, OH) and the Instrument Center of the Department of Chemistry at the University at Buffalo. Compounds **I** and **XI** were prepared as previously described.¹⁰

Liposome Samples Preparation. The lipid was layered at the bottom of a vial by evaporating the ethanol solvent under nitrogen. Diethyl ether was added, and the solution was thoroughly re-evaporated to complete dryness. After addition of buffer, the sample was vortexed for 3 min and then sonicated for 15 min, at 4 °C, by a probe sonicator (MSE, Crawley, U.K.) until a clear sample was obtained. This suspension was the stock suspension of unilamellar liposomes, as confirmed by electron microscopy. For all the photosensitizers but **I**, we found that the binding to liposomes, when the dye was added from a concentrated stock solution in DMSO, was very slow (more than 48 h). Thus, to obtain inclusion of all the molecules, other than **I**, in the bilayer membrane, for ¹O₂ quantum yield measurements, we added the dyes to the lipid solution in ethanol prior to sonication and continued with the procedure described above and csonicated the dye with the lipids.

For fluorescence resonance energy transfer (FRET) measurements, we prepared liposomes from 1,2-dimyristoyl-*sn*-glycero-3-phosphocholine (DMPC, 99%) and dansyl-DHPE (which served as the donor-labeled lipid) in a molar ratio of 9:1, respectively. Chloroform was added to the mixed lipid powder of DMPC and dansyl-DHPE, and the solution was evaporated to complete dryness. Buffer was added to the dried lipids, and the sample was vortexed for 3 min and then sonicated for 10 min, at 4 °C, by a probe sonicator. The solution was then divided into seven vials, and the dithiaporphyrins, which were the acceptors, were added to six vials. All the samples were resonicated for another 10 min, at 4 °C, to incorporate the dithiaporphyrins.

General Procedure for the Preparation of Ethyl Carboxylatoalkoxy Dithiaporphyrins XII–XVI. *Preparation of Ethyl 5,20-Diphenyl-10,15-bis-(4-carboxylatopropanoxy)phenyl-21,23-dithiaporphyrin (XII).* Core-modified porphyrin **XI** (0.36 g, 0.53 mmol), 0.73 g of K₂CO₃, and 0.8 mL of ethyl bromobutanoate in 50 mL of acetone were heated at reflux for 15 h. The reaction mixture was cooled to ambient temperature, and the K₂CO₃ was removed by filtration. The filter cake was washed with acetone until the filtrate was colorless. The combined filtrates were concentrated. The crude product was washed with MeOH to give 0.42 g (87%) of **XII** as a purple solid; mp 120–122 °C. ¹H NMR (CDCl₃, 400 MHz) δ 1.35 (6H, t, *J* = 7.1 Hz), 2.13–2.22 (4H, m), 2.70 (4H, t, *J* = 7.2 Hz), 4.25 (4H, q, *J* = 7.1 Hz), 4.31 (4H, t, *J* = 6.0 Hz), 7.33 (4H, d, *J* = 6.4 Hz), 7.75–7.85 (6H, m), 8.16 (4H, d, *J* = 6.4 Hz), 8.20–8.30 (4H, m), 8.70 (4H, dd, *J* = 13.1, 4.5 Hz), 9.67 (2H, s), 9.72 (2H, s). ¹³C NMR (CDCl₃, 400 MHz) δ 14.7, 25.2, 31.3, 60.9, 67.4, 113.9, 127.7, 128.3, 134.1, 134.1, 134.3, 134.5, 134.7, 134.9, 135.7, 135.7, 135.8, 141.6, 148.0, 148.4, 156.7, 157.0, 159.4, 173.7. High-resolution Q-TOF MS: *m/z* 909.3027 (calcd for C₅₆H₄₈N₂O₆S₂ + H, 909.3032).

Preparation of Ethyl 5,20-Diphenyl-10,15-bis-(4-carboxylatobutoxy)phenyl-21,23-dithiaporphyrin (XIII). Core-modified porphyrin **XI** (0.36 g, 0.53 mmol), 0.73 g of K₂CO₃, and 0.8 mL of ethyl bromopentanoate in 50 mL of acetone were treated as described for the preparation of **XII** to give 0.40 g (81%) of **XIII** as a purple solid; mp 192–194 °C. ¹H NMR (CDCl₃, 400 MHz) δ 1.33 (6H, t, *J* = 7.1), 1.97–2.09 (4H, m), 2.53 (4H, t, *J* = 6.7 Hz), 4.22 (4H, q, *J* = 7.1 Hz), 4.28 (4H, t, *J* = 5.5

Hz), 7.34 (4H, d, $J = 6.3$ Hz) 7.78–7.85 (6H, m), 8.16 (4H, d, $J = 6.3$ Hz), 8.25 (4H, dd, $J = 7.3, 1.5$ Hz), 8.68 (2H, d, $J = 3.4$ Hz), 8.71 (2H, d, $J = 3.4$ Hz), 9.67 (2H, s), 9.72 (2H, s). ^{13}C NMR (CDCl_3 , 400 MHz) δ 14.7, 22.2, 29.2, 34.4, 60.8, 68.1, 113.9, 127.7, 128.3, 134.0, 134.1, 134.4, 134.5, 134.7, 134.9, 135.6, 135.8, 141.6, 148.0, 148.5, 156.7, 157.0, 159.5, 173.9. High-resolution Q-TOF MS: m/z 937.3378 (calcd for $\text{C}_{58}\text{H}_{52}\text{N}_2\text{O}_6\text{S}_2 + \text{H}$, 937.3345).

Preparation of Ethyl 5,20-Diphenyl-10,15-bis-(4-carboxylatopentoxo)phenyl-21,23-dithiaporphyrin (XIV). Core-modified porphyrin **XI** (0.38 g, 0.56 mmol), 0.77 g of K_2CO_3 , and 1.0 mL of ethyl bromohexanoate in 50 mL of acetone were treated as described for the preparation of **XII** to give 0.48 g (89%) of **XIV** as a purple solid; mp 190–192 °C. ^1H NMR (CDCl_3 , 400 MHz) δ 1.32 (6H, t, $J = 7.1$ Hz), 1.65–1.74 (4H, m), 1.81–1.90 (4H, m), 1.96–2.06 (4H, m), 2.45 (4H, t, $J = 7.5$ Hz), 4.20 (4H, q, $J = 7.1$ Hz), 4.25 (4H, t, $J = 6.3$ Hz), 7.33 (4H, d, $J = 6.4$ Hz), 7.77–7.85 (6H, m), 8.16 (4H, d, $J = 6.4$ Hz), 8.25 (4H, dd, $J = 7.2, 1.6$ Hz), 8.68 (2H, d, $J = 3.4$ Hz), 8.72 (2H, d, $J = 3.4$ Hz), 9.67 (2H, s), 9.73 (2H, s). ^{13}C NMR (CDCl_3 , 400 MHz) δ 14.7, 25.2, 26.2, 29.5, 34.7, 60.7, 68.3, 113.9, 127.7, 128.3, 133.9, 134.1, 134.4, 134.5, 134.7, 134.9, 135.6, 135.8, 141.7, 148.0, 148.5, 156.7, 157.0, 159.6, 174.1. High-resolution Q-TOF MS: m/z 965.3676 (calcd for $\text{C}_{60}\text{H}_{56}\text{N}_2\text{O}_6\text{S}_2 + \text{H}$, 965.3658).

Preparation of Ethyl 5,20-Diphenyl-10,15-bis-(4-carboxylatohexoxy)phenyl-21,23-dithiaporphyrin (XV). Core-modified porphyrin **XI** (0.38 g, 0.56 mmol), 0.77 g of K_2CO_3 , and 1.1 mL of ethyl bromopentanoate in 50 mL of acetone were treated as described for the preparation of **XII** to give 0.48 mg (87%) of **XV** as a purple solid; mp 173–175 °C. ^1H NMR (CDCl_3 , 400 MHz) δ 1.31 (6H, t, $J = 7.13$ Hz), 1.46–1.58 (4H, m), 1.61–1.71 (4H, m), 1.72–1.82 (4H, m), 1.93–2.04 (4H, m), 2.41 (4H, t, $J = 7.5$ Hz), 4.19 (4H, q, $J = 7.1$ Hz), 4.25 (4H, t, $J = 6.4$ Hz), 7.34 (4H, d, $J = 6.4$ Hz), 7.73–7.85 (6H, m), 8.17 (4H, d, $J = 6.4$ Hz), 8.26 (4H, dd, $J = 7.1, 1.5$ Hz), 8.68 (2H, d, $J = 3.4$ Hz), 8.73 (2H, d, $J = 3.4$ Hz), 9.67 (2H, s), 9.74 (2H, s). ^{13}C NMR (CDCl_3 , 400 MHz) δ 14.7, 25.3, 26.3, 29.4, 29.6, 34.7, 60.6, 68.5, 113.9, 127.7, 128.3, 133.9, 134.1, 134.4, 134.5, 134.7, 134.9, 135.6, 135.8, 141.7, 148.0, 148.5, 156.7, 157.0, 159.6, 174.2. High-resolution Q-TOF MS: m/z 993.3991 (calcd for $\text{C}_{62}\text{H}_{60}\text{N}_2\text{O}_6\text{S}_2 + \text{H}$, 993.3971).

Preparation of Ethyl 5,20-Diphenyl-10,15-bis-(4-carboxylatodecocy)phenyl-21,23-dithiaporphyrin (XVI). Core-modified porphyrin **XI** (0.38 mg, 0.56 mmol), 0.8 g of K_2CO_3 , and 1.4 mL of ethyl bromoundecanoate in 50 mL of acetone were treated as described for the preparation of **XII** to give 0.55 g (89%) of **XVI** as a purple oil. ^1H NMR (CDCl_3 , 400 MHz) δ 1.10–1.35 (22H, m), 1.58–1.70 (4H, m), 1.73–1.83 (4H, m), 1.84–1.94 (4H, m), 2.05–2.16 (4H, m), 2.29 (4H, t, $J = 7.5$ Hz), 4.13 (4H, q, $J = 7.1$ Hz), 4.36 (4H, t, $J = 6.4$ Hz), 7.34 (4H, d, $J = 6.4$ Hz), 7.78–7.82 (6H, m), 8.16 (4H, d, $J = 6.40$ Hz), 8.25 (4H, dd, $J = 7.0, 1.5$ Hz), 8.67 (2H, d, $J = 3.4$ Hz), 8.72 (2H, d, $J = 3.4$ Hz), 9.66 (2H, s), 9.73 (2H, s). High-resolution Q-TOF MS: m/z 1105.5253 (calcd for $\text{C}_{70}\text{H}_{76}\text{N}_2\text{O}_6\text{S}_2 + \text{H}$, 1105.5223).

General Procedure for Saponification of Ethyl Esters of Dithiaporphyrins. Preparation of 5,20-Diphenyl-10,15-bis-(4-carboxylatopropanoxy)phenyl-21,23-dithiaporphyrin (**III**). Core-modified porphyrin **XII** (0.25 g, 0.27 mmol) was dissolved in 30 mL of tetrahydrofuran (THF), and 30 mL of 1.0 M aqueous NaOH was added. The resulting solution was stirred at ambient temperature for 15 h. The solution was acidified by the addition of 3.3 mL of concentrated HCl (36%). The reaction mixture

was diluted with 200 mL of H_2O , and the products were extracted with EtOAc (3×200 mL). The combined organic extracts were dried over MgSO_4 and concentrated. The crude product was washed with several portions of hexanes/MeOH to give 0.20 g (85%) of **III** as a purple solid; mp 282–284 °C. ^1H NMR ($\text{CDCl}_3/\text{CD}_3\text{OD}$, 400 MHz) δ 2.19–2.29 (4H, m), 2.64 (4H, t, $J = 7.2$ Hz), 4.24 (4H, t, $J = 6.1$ Hz), 7.27 (4H, d, $J = 6.5$ Hz), 7.72–7.76 (6H, m), 8.10 (4H, d, $J = 6.4$ Hz), 8.17–8.20 (4H, m), 8.64 (4H, dd, $J = 13.6, 4.5$ Hz), 9.63 (2H, s), 9.68 (2H, s). ^{13}C NMR ($\text{CDCl}_3/\text{CD}_3\text{OD}$, 400 MHz) δ 26.0, 31.9, 68.3, 114.8, 128.7, 129.3, 134.9, 135.1, 135.3, 135.4, 135.6, 135.8, 136.7, 142.4, 148.9, 149.3, 157.7, 157.9, 160.3, 177.2. High-resolution Q-TOF MS: m/z 853.2357 (calcd for $\text{C}_{52}\text{H}_{40}\text{N}_2\text{O}_6\text{S}_2 + \text{H}$, 853.2406). Anal. Calcd for $\text{C}_{52}\text{H}_{40}\text{N}_2\text{O}_6\text{S}_2 \cdot \text{CH}_3\text{OH}$: C, 71.31; H, 5.15; N, 3.11. Found: C, 71.25; H, 5.47; N, 2.65.

Preparation of 5,20-Diphenyl-10,15-bis-(4-carboxylatobutoxy)phenyl-21,23-dithiaporphyrin (IV). Core-modified porphyrin **XIII** (0.25 g, 0.27 mmol) in 30 mL of THF was treated with 20 mL of 1.0 M aqueous NaOH as described for the preparation of **III** to give 0.19 g (81%) of core-modified porphyrin **IV** as a purple solid; mp 153–155 °C. ^1H NMR (CDCl_3 , 400 MHz) δ 1.90–1.98 (8H, m), 2.49–2.57 (4H, m), 4.06–4.12 (4H, m), 7.20 (4H, d, $J = 6.2$ Hz), 7.72–7.80 (6H, m), 8.08 (4H, d, $J = 6.3$ Hz), 8.22 (4H, dd, $J = 6.2, 1.8$ Hz), 8.66 (2H, d, $J = 3.4$ Hz), 8.68 (2H, d, $J = 3.4$ Hz), 9.66 (2H, s), 9.69 (2H, s). ^{13}C NMR (CDCl_3 , 400 MHz) δ 21.9, 29.0, 34.0, 67.9, 113.8, 127.7, 128.3, 133.9, 134.1, 134.4, 134.5, 134.7, 134.9, 135.7, 135.7, 141.6, 148.0, 148.5, 156.7, 156.9, 159.3, 179.7. High-resolution Q-TOF MS: m/z 881.2739 (calcd for $\text{C}_{54}\text{H}_{44}\text{N}_2\text{O}_6\text{S}_2 + \text{H}$, 881.2719). Anal. Calcd for $\text{C}_{54}\text{H}_{44}\text{N}_2\text{O}_6\text{S}_2 \cdot \text{CH}_3\text{OH}$: C, 72.34; H, 5.30; N, 3.07. Found: C, 72.33; H, 5.07; N, 2.91.

Preparation of 5,20-Diphenyl-10,15-bis-(4-carboxylatopentoxo)phenyl-21,23-dithiaporphyrin (V). Core-modified porphyrin **XIV** (0.25 g, 0.26 mmol) in 30 mL of THF was treated with 20 mL of 1.0 M aqueous NaOH as described for the preparation of **III** to give 0.20 g (85%) of core-modified porphyrin **V** as a purple solid; mp 184–186 °C. ^1H NMR ($\text{CDCl}_3/\text{CD}_3\text{OD}$, 400 MHz) δ 1.60–1.72 (4H, m), 1.74–1.86 (4H, m), 1.91–2.02 (4H, m), 2.43 (4H, t, $J = 7.5$ Hz), 4.22 (4H, t, $J = 6.3$ Hz), 7.30 (4H, d, $J = 6.4$ Hz), 7.70–7.82 (6H, m), 8.13 (4H, d, $J = 6.4$ Hz), 8.67 (4H, dd, $J = 17.0, 4.5$ Hz), 8.79 (2H, d, $J = 3.4$ Hz), 8.83 (2H, d, $J = 3.4$ Hz), 9.65 (2H, s), 9.70 (2H, s). ^{13}C NMR ($\text{CDCl}_3/\text{CD}_3\text{OD}$, 400 MHz) δ 25.7, 26.8, 30.1, 34.9, 69.0, 114.5, 128.4, 129.0, 134.5, 134.7, 135.1, 135.1, 135.3, 135.5, 136.3, 136.4, 142.2, 148.6, 149.1, 157.3, 157.6, 160.2, 177.4. High-resolution Q-TOF MS: m/z 909.3003 (calcd for $\text{C}_{56}\text{H}_{48}\text{N}_2\text{O}_6\text{S}_2 + \text{H}$, 909.3032). Anal. Calcd for $\text{C}_{56}\text{H}_{48}\text{N}_2\text{O}_6\text{S}_2$: C, 73.98; H, 5.32; N, 3.08. Found: C, 74.11; H, 5.23; N, 3.08.

Preparation of 5,20-Diphenyl-10,15-bis-(4-carboxylatohexoxy)phenyl-21,23-dithiaporphyrin (VI). Core-modified porphyrin **XV** (0.25 g, 0.25 mmol) in 30 mL of THF was treated with 20 mL of 1.0 M aqueous NaOH as described for the preparation of **III** to give 0.20 g (85%) of core-modified porphyrin **VI** as a purple solid; mp 105–107 °C. ^1H NMR (CDCl_3 , 400 MHz) δ 1.45–1.58 (4H, m), 1.58–1.70 (4H, m), 1.70–1.83 (4H, m), 1.86–2.01 (4H, m), 2.45 (4H, t, $J = 7.4$ Hz), 4.17 (4H, t, $J = 5.6$ Hz), 7.27 (4H, d, $J = 6.3$ Hz), 7.76–7.81 (6H, m), 8.13 (4H, d, $J = 6.3$ Hz), 8.24 (4H, dd, $J = 6.8, 1.4$ Hz), 8.67 (2H, d, $J = 3.4$ Hz), 8.72 (2H, d, $J = 3.4$ Hz), 9.66 (2H, s), 9.71 (2H, s). ^{13}C NMR (CDCl_3 , 400 MHz) δ 25.0, 26.2, 29.2, 29.4, 30.1, 34.3, 68.3, 113.9, 127.7, 128.3, 133.8, 134.1, 134.5, 134.7, 134.9, 135.6, 135.8, 141.6, 148.0, 148.5, 156.7, 156.9, 159.5,

179.9. High-resolution Q-TOF MS: m/z 937.3354 (calcd for $C_{58}H_{52}N_2O_6S_2 + H$, 937.3345). Anal. Calcd for $C_{58}H_{52}N_2O_6S_2$: C, 72.63; H, 5.90; N, 2.73. Found: C, 72.54; H, 6.02; N, 2.44.

Preparation of 5,20-Diphenyl-10,15-bis-(4-carboxylatodecoxy)phenyl-21,23-dithiaphorphyrin (X). Core-modified porphyrin **XVI** (0.25 g, 0.23 mmol) in 30 mL of THF was treated with 10 mL of 1.0 M aqueous NaOH as described for the preparation of **III** to give 0.18 g (76%) of core-modified porphyrin **X** as a purple solid; mp 123–125 °C. 1H NMR ($CDCl_3$, 400 MHz) δ 1.30–1.51 (20H, m), 1.56–1.64 (4H, m), 1.64–1.72 (4H, m), 1.90–2.00 (4H, m), 2.40 (4H, t, $J = 7.4$ Hz), 4.20 (4H, t, $J = 6.4$ Hz), 7.31 (4H, d, $J = 6.3$ Hz), 7.74–7.84 (6H, m), 8.15 (4H, d, $J = 6.3$ Hz), 8.25 (4H, dd, $J = 7.6$, 2.3 Hz), 8.68 (2H, d, $J = 3.4$ Hz), 8.72 (2H, d, $J = 3.4$ Hz), 9.67 (2H, s), 9.72 (2H, s). ^{13}C NMR ($CDCl_3$, 400 MHz), 25.0, 26.5, 29.4, 29.6, 29.7, 29.9, 34.4, 68.6, 113.9, 127.7, 128.3, 133.8, 134.1, 134.5, 134.5, 134.7, 134.9, 135.6, 135.8, 141.6, 148.0, 148.5, 156.7, 156.9, 159.6, 180.2. High-resolution Q-TOF MS: m/z 1049.4609 (calcd for $C_{66}H_{68}N_2O_6S_2 + H$, 1049.4597). Anal. Calcd for $C_{66}H_{68}N_2O_6S_2 \cdot CH_3OH$: C, 74.41; H, 6.71; N, 2.59. Found: C, 74.72; H, 7.11; N, 2.53.

Photophysical Properties. Spectroscopic Measurements. Absorption spectra were recorded on a Shimadzu (Kyoto, Japan) UV-2501PC UV–vis spectrophotometer and on a Perkin-Elmer (Norwalk, CT) UV–vis–near-IR Lambda 12 spectrophotometer. Fluorescence excitation and emission spectra, fluorescence time-drive measurements, and FRET measurements were performed on a Perkin-Elmer LS-50B digital fluorimeter. For all fluorescence measurements, the sample's optical density was maintained below 0.05 at the wavelength of fluorescence excitation in order to establish a linear dependence of the fluorescence intensity on concentration.

Fluorescence Resonance Energy Transfer Measurements in Liposomes. FRET involves energy transfer from the excited state of a donor (dansyl-DHPE in this case) to a suitable acceptor (the photosensitizers **I**, **III**, **IV**, **V**, **VI**, and **X**), through a nonradiative dipole–dipole interaction.^{16–20} For the donor/acceptor pair, the excitation wavelength was set at 336 nm (the absorbance peak of the donor). At this wavelength the acceptor has no absorbance. The emission spectra were collected in the spectral range from 370 to 800 nm. FRET was measured in liposomes containing known concentrations of donor-labeled lipids and the sensitizers as acceptors. Liposomes containing only donor-labeled lipids served as the “donor-only” control. The dansyl-DHPE architecture leaves the dansyl moiety in the surface of the bilayer close to the aqueous phase. We used the fact that the donor has a fixed position in the liposome, to find the positions of the different photosensitizers (acceptors) in the bilayer, using the FRET effect.

The fraction of light intensity emitted by the donor that is transferred to the acceptor, termed the energy transfer efficiency E , is dependent on the distance between the donor and acceptor, R :

$$E = \frac{1}{1 + (R/R_0)^6} \quad (1)$$

where R_0 is the Förster distance of this pair of donor and acceptor at which the FRET efficiency is 50%. E was calculated from measurements of donor emission intensity at 550 nm (where the acceptor does not emit) in the absence and presence of the acceptor according to

$$E = 1 - \frac{I_{DA}}{I_D} \quad (2)$$

where I_D and I_{DA} are the donor emission intensities of samples containing only donor and samples with both donor and acceptor, respectively.

Measurements of 1O_2 Quantum Yields (Φ_Δ) in Methanol and Liposomes. The reaction mixture consisted of the organic solvent, methanol, or the microsolvent, namely, liposomes, the sensitizer and 9,10-dimethylantracene (DMA). DMA (at 5 μ M concentration, added from a 2 mM stock solution in DMF) was employed to trap 1O_2 , since it reacts rapidly (with a rate constant $= 2 \times 10^7$ to 9×10^8 $M^{-1} s^{-1}$)²¹ and selectively with it in many organic solvents and also in water, to form the 9,10-endoperoxide (DMAO₂).^{22–24} We performed in situ fluorescence measurements of DMA, using standard 90° geometry, in a time-drive mode, while the laser beam at 514.5 nm for the measurements in methanol and 454.5 nm for the measurements in liposomes (Coherent Innova 200 Ar⁺, Palo Alto, CA) transverses the sample cuvette and excites the dithiaphorphyrin sensitizer. The power level at the entry point to the solution was ~ 6 mW. Constancy of the laser power during the experiments was verified at the sample surface with a power meter (model PD2-A, Ophir, Jerusalem, Israel). No self-sensitization or bleaching of the photosensitizers themselves or of DMA without sensitizer was observed. The production rate of excited photosensitizer, in molar concentration/s, k_{pho} , is given by the following equation:²⁵

$$k_{pho} = \frac{0.98P(1 - 10^{(-absL)})}{EV} \quad (3)$$

where P is the laser power (in mW), abs is the optical density/cm, L is the sample length along the laser beam's axis, in centimeters, E is the number of Einstein units (1 Einstein = 6.023×10^{23} photons) per second per watt of light, and V is the sample volume (in mL). The factor “0.98” corrects for the light reflected at the air/sample interface, using Fresnel equations of reflection.

The time-dependent fluorescence intensity of DMA was excited at 377 nm and measured at 429 nm. DMA's fluorescence disappearance followed first-order kinetics according to the following equation:

$$DMA_{flu} = Ae^{-k_{DMA} \text{time}} \quad (4)$$

where k_{DMA} is the rate constant for the decrease in DMA fluorescence, DMA_{flu} . The program Origin (Microcal Software, Northampton, MA) was used for curve-fitting and extraction of k_{DMA} . The singlet oxygen quantum yield is proportional to the value of (k_{DMA}/k_{pho}) , where k_{pho} (eq 3) is the rate constant for either the sensitizer or a known standard. Rose bengal ($\Phi_{\Delta, \text{stand}} = 0.80$)²⁶ and hematoporphyrin ($\Phi_{\Delta, \text{stand}} = 0.75$) were used as standards for the organic and membrane measurements, respectively. Unbound DMA, i.e., the water fraction, does not interfere with the measurements of Φ_Δ in liposomes since the ratio of DMA fluorescence in water versus liposome is vanishingly small.²⁵ Knowing $\Phi_{\Delta, \text{stand}}$ of the standard, $\Phi_{\Delta, \text{sens}}$ for the studied sensitizer was determined using the following expression:

$$\frac{\Phi_{\Delta, \text{sens}}}{\Phi_{\Delta, \text{stand}}} = \frac{\left(\frac{k_{\text{DMA}}}{k_{\text{pho}}}\right)_{\text{sens}}}{\left(\frac{k_{\text{DMA}}}{k_{\text{pho}}}\right)_{\text{stand}}} \quad (5)$$

Measurements of Binding Constants, K_b . We found that the longer the side chain on the dithiaporphyrin the slower it binds to liposomes. Due to the slow binding of all the photosensitizers except **I**, we performed binding measurements to liposomes only on **I**. The fluorescence intensity of **I** was monitored in aqueous solution upon addition of increasing amounts of liposomes from their stock suspension. Following each added batch, a 5 min incubation period was found to be sufficient to achieve equilibrated binding.

Estimates of the Mean and Error for Φ_{Δ} and K_b . The values for Φ_{Δ} and K_b were determined by statistically averaging two to five independent measurements. The weighted average, μ , of several measurements, each yielding a result x_i and possessing a measurement error σ_i , was calculated using the formula²⁷

$$\mu = \frac{\sum (x_i/\sigma_i^2)}{\sum (1/\sigma_i^2)} \quad (6)$$

The uncertainty of the calculated average, σ_{μ} , is estimated by²⁷

$$\sigma_{\mu}^2 = \frac{1}{\sum (1/\sigma_i^2)} \quad (7)$$

Biological Properties. Cell Cultures. U937 human leukemic monocytic cells were cultured in humidified atmosphere containing 5% CO₂, in RPMI 1640 medium (Biological Industries, Israel), supplemented with 10% fetal bovine serum (FBS) (Biological Industries, Israel), 2 mM L-glutamine, 10 mM Hepes buffer solution, 1 mM sodium pyruvate, 50 units/mL penicillin G, and 50 µg/mL streptomycin.

R3230AC rat mammary adenocarcinoma cells were cultured in humidified atmosphere containing 5% CO₂, in minimum essential medium (α-MEM) supplemented with 10% FBS, 50 units/mL penicillin G, 50 µg/mL streptomycin, and 1.0 µg/mL Fungizone (complete medium).

PDT Treatment. U937 cells at 5×10^5 cells/mL were grown in cell culture flasks and incubated for 2 h with, or without, photosensitizer (0.5 µM) in subdued light conditions at 37 °C. The cells were then transferred to a 96-well plate, and the plates were illuminated with light intensity of 2.5 mW cm⁻² for various times with a fluorescence tube (Phillips type super actinic TLD 15W/03), with illumination band of 380–480 nm. The cells were incubated for 20 h after illumination and then tested for cytotoxicity. Cell viability was assessed by trypan blue exclusion (0.5% trypan blue in PBS for 4 min). A viable cell excludes an acidic dye, such as trypan blue; therefore, its uptake is indicative of irreversible membrane damage preceding cell death.

R3230AC cells were seeded on 96-well plates at $(1-1.5) \times 10^4$ cells/well in complete medium. Cultures were then incubated for 24 h after which the appropriate concentrations of **I**, **III**, **IV**, **V**, **VI**, or **X** were added directly to the wells in the complete medium. Cells were illuminated for 45 min with broad-band visible light (350–750 nm) delivered at 1.4 mW cm⁻² from a filtered 750 W halogen source defocused to encompass the whole 96-well plate. The clear medium was then removed, 0.2 mL of fresh complete medium was added, and the cultures were incubated at 37 °C for 24 h in the dark. Cell monolayers were

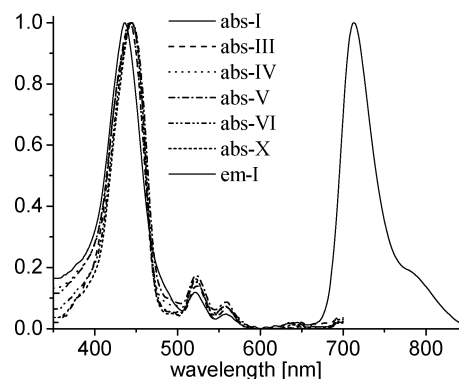


Figure 2. Absorption spectra of all the photosensitizers and a representative emission spectrum (**I**). All emission spectra are similar to the emission spectrum of **I**, with very small deviations (<3 nm) in peak locations.

TABLE 1: UV–Vis Band Maxima and Molar Absorptivities for the Different Photosensitizers, in THF, λ_{max} nm ($\epsilon \times 10^3$ M⁻¹ cm⁻¹)

	Soret	band 1	band 2	band 3	band 4
TPPS₄ ^a	411 (464)	513 (15.5)	549 (7.0)	577 (6.5)	630 (3.9)
I ^b	435 (314)	513 (27.7)	549 (10.7)	632 (3.2)	698 (7.0)
III	438 (224)	516 (25.0)	551 (10.6)	636 (1.9)	700 (5.9)
IV	438 (157)	516 (19.5)	551 (8.6)	636 (1.5)	700 (4.6)
V	438 (110)	516 (20.3)	551 (8.8)	636 (1.6)	700 (5.0)
VI	438 (90.6)	516 (18.4)	551 (8.1)	635 (1.5)	700 (4.5)
X	438 (314)	516 (24.8)	552 (10.8)	636 (1.9)	700 (6.0)

^a Data from ref 13. ^b Data from ref 10.

also maintained in the dark, undergoing the same medium changes and addition of dyes as those that were illuminated. Cell viability was determined using the MTT assay.²⁸

Dark and Phototoxicity. Cytotoxicity in U937 cells was determined by the trypan blue exclusion test. Cells were loaded with 0.4% trypan blue on a hemacytometer slide at the ratio 1:1 (v/v) and analyzed by light microscopy. The percentage of dead cells was determined by counting a total of 200 cells per independent experiment.

Results and Discussion

Spectroscopic Measurements. The structural variations among **I**, **III**, **IV**, **V**, **VI**, and **X** have little effect on their absorption and emission spectra, which were quite similar to those of compound **I**. Values of band maxima and molar absorptivities are compiled in Table 1. A maximum red shift of 3 nm was observed in the main peak of fluorescence for **X** (Figure 2).

The dithiaporphyrins have similar absorbance bands to those of the corresponding porphyrins. This is illustrated in Table 1 for tetraphenylporphyrin tetrasulfonate (**TPPS₄**), which has been used as a photosensitizer both in vitro and in vivo.¹ As shown in Table 1, the dithiaporphyrins have longer-wavelength-absorbing band 3 and band 4 maxima than **TPPS₄**, but more importantly, have band 4 molar extinction coefficients, ϵ , that are in the 4500–7000 M⁻¹ cm⁻¹ range, which are significantly higher than the band 4 absorbance of **TPPS₄**, with ϵ of 3900 M⁻¹ cm⁻¹. The band 4 absorbances of the dithiaporphyrins are also significantly higher than those for the clinically viable photosensitizers Photofrin II (band 4 λ_{max} of 630 nm, ϵ of 1170 M⁻¹ cm⁻¹) and protoporphyrin IX (band 4 λ_{max} of 635 nm, ϵ of <5000 M⁻¹ cm⁻¹).¹ Although values of ϵ are important for light harvesting, the localization of the photosensitizer ultimately determines the effectiveness of the photosensitizer.¹

TABLE 2: Energy Transfer Efficiency, Measured in Liposomes for the Different Donor/Acceptor Pairs^a

photosensitizer	I	III	IV	V	VI	X
energy transfer efficiency [%]	56.9 ± 1.1	34.2 ± 0.7	28.2 ± 0.6	17.6 ± 0.4	12.0 ± 0.4	7.9 ± 0.2

^a In all cases the donor is dansyl attached to the headgroup of DHPE and is positioned in the surface of the bilayer, at the lipid/aqueous interface.

Binding of I to Liposomes. Liposomes composed of naturally extracted lecithin have structures similar to those of biological membranes.²⁹ This fact suggests that lecithin liposomes are a good model for cellular membranes. However, measurements using liposomes differ from those of cellular membranes, since liposomes do not show the effect of membrane-bound proteins, their active transport functionality, and other properties. These differences render liposome-binding information somewhat less relevant for cellular and in vivo processes, and therefore, liposomes are only approximate models of membranes.

We attempted to measure the binding of the photosensitizers to liposomes in order to find the binding constant, K_b . In all cases, except with **I**, very slow binding (more than 48 h) to the liposomes rendered it impossible to calculate K_b .

For the measurement of K_b for **I**, we employed the changes that are observed in intensity of the emission spectrum of **I** upon its partitioning into a lecithin environment. The ratio between the fluorescence intensity of the dye that is measured in the presence of increasing amounts of lipid, F_{obs} , and the initial intensity that was measured in an aqueous solution, F_{init} , depends on lipid concentration as follows:³⁰

$$\frac{F_{\text{obs}}}{F_{\text{init}}} = \frac{F_{\infty}}{F_{\text{init}}} - \frac{(F_{\text{obs}}/F_{\text{init}}) - 1}{K_b[\text{lpd}]} \quad (8)$$

where [lpd] is the lipid concentration and F_{∞} is the fluorescence intensity of the dye at complete binding. Algebraic manipulation results in the hyperbolic function:

$$F_{\text{obs}} = \frac{F_{\text{init}} + F_{\infty}K_b[\text{lpd}]}{1 + K_b[\text{lpd}]} \quad (9)$$

The calculated binding constant of **I** to liposomes is $K_b = 23.3 \pm 1.6 \text{ (mg/mL)}^{-1}$. The binding of **I** into the lipid environment, which is faster than for the other photosensitizers, may be somewhat surprising considering the longer side chains and hence the higher hydrophobicity of the other dithiaporphyrins. Furthermore, we tested all photosensitizers for aggregation and found no aggregation at concentrations up to 2 μM , which suggests that aggregation of the more hydrophobic sensitizers is not responsible for the slower binding to liposomes. In addition, the uptake measurements in cells clearly show that all the photosensitizers penetrate the cells. A possible reason for the differences in the in vitro and in vivo results was outlined above, viz., the incomplete biological relevance of liposome models, and mainly the endocytosis mechanism in the cell.

FRET Measurements. In the Ehrenberg lab we usually employ fluorescence quenching measurements with either iodide ions or spin-probe-labeled lipids to determine the depth of the photosensitizer in the membrane.^{31–35} In this work we could quench the photosensitizers neither by iodide nor by other known quenchers. Therefore, we applied FRET as a special and interesting method to measure the photosensitizers' depth in the membrane. FRET involves energy transfer from the excited state of the donor (dansyl-DHPE) to the acceptor (the photosensitizer), through a nonradiative dipole–dipole interaction. Figure 3 demonstrates the FRET effect. The experiment was repeated three times and showed the same results. Using eq 2 we

calculated the energy transfer efficiency for all the donor/acceptor pairs (Table 2). As can be seen, as the side chain becomes longer, the energy transfer efficiency decreases. For **I** with the shortest side chain (only one methylene carbon), we measured energy transfer efficiency of about 57%, whereas for **X**, whose side chain is the longest (10 carbons), the energy transfer efficiency was approximately 8%. From the relationship between energy transfer efficiency and donor–acceptor distance (eq 1), we conclude that as the side chain becomes longer, the photosensitizer is further removed from the surface of the bilayer. From this conclusion we visualize the photosensitizers being positioned in the bilayer with their acid tails at the interface with the water, while their hydrophobic core is found deeper in the bilayer.

Production of Singlet Oxygen (¹O₂) in Methanol and in Liposomes. The ability to produce singlet oxygen is a very important requirement from a potential photosensitizer for PDT. The quantum yield for the generation of ¹O₂, Φ_{Δ} , by **I** in methanol was measured previously by a direct methods.^{10,36} This measurement showed high quantum yield in methanol (0.8) and encouraged us to test molecules with similar structure as photosensitizers for PDT. We calculated the quantum yield of all the photosensitizers indirectly, by measuring the photooxidation efficiency of a singlet oxygen target and using rose bengal as a standard sensitizer, having $\Phi_{\Delta, \text{stand}} = 0.80$,²⁶ as described in the Materials and Methods section. All photosensitizers showed a very high quantum yield (around 1) in methanol (Figure 4). These values are higher than the singlet oxygen quantum yield measured for Photofrin II,³⁷ which is an approved photosensitizer for several clinical protocols.¹

Quantum yields for the generation of ¹O₂ by the photosensitizers were also determined in liposomes by using the lipophilic DMA singlet oxygen trap (as in methanol), whose reaction is rapid, and it binds to liposomes efficiently, $K_b = 2.7 \text{ (mg/mL)}^{-1}$.^{25,38} Since all molecules but **I** showed very slow binding to liposomes, all molecules were incorporated in L- α -lecithin by cosonication. The calculated values of Φ_{Δ} of liposome-bound photosensitizers were significantly lower than the values of Φ_{Δ} in methanol (Figure 4). The photosensitizers possessing short

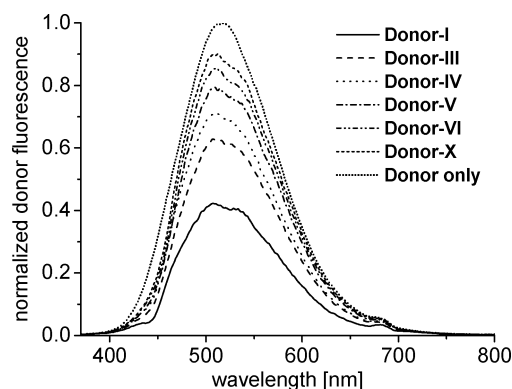


Figure 3. Set of spectra demonstrating the FRET effect. The excitation wavelength for all samples was fixed at 336 nm so that only the donor (dansyl-DHPE) was directly excited. FRET results in the decrease of donor fluorescence in the presence of acceptor. The closer the acceptor is to the donor the higher is the decrease in the donor fluorescence intensity.

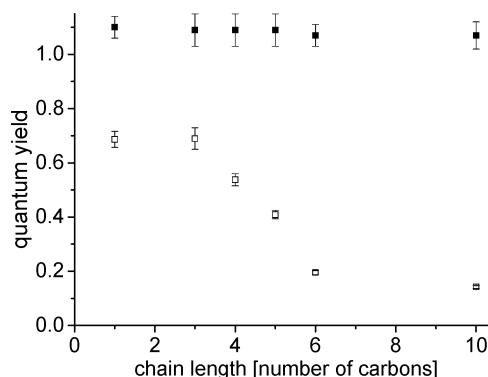


Figure 4. Quantum yields for the generation of singlet oxygen, Φ_{Δ} , in methanol (filled squares) and in liposomes (hollow squares).

TABLE 3: Quantum Yields for the Generation of $^1\text{O}_2$ by **III and **VI** in Liposomes as a Function of the Photosensitizer's Concentration**

	0.5 μM	1 μM	2 μM	3 μM	5 μM
III	0.64 ± 0.07	0.69 ± 0.04	0.66 ± 0.03	0.48 ± 0.01	0.485 ± 0.004
VI	0.25 ± 0.02	0.2 ± 0.01	0.179 ± 0.002	0.151 ± 0.001	0.146 ± 0.001

side chains (**I** and **III**) showed high quantum yields, around 0.7, whereas the photosensitizers possessing longer side chains showed decreasing quantum yields between 0.54 for **IV** to 0.15 for **X**. From these results we might assume that as the side chain becomes longer, the molecule is positioned in a shallower location in the membrane and thus singlet oxygen escapes the membrane before it induces damage.³¹ But the previously discussed FRET results contradict this assumption and show that the long-chain molecules are positioned deeper in the bilayer.

The generation of $^1\text{O}_2$ involves collisional transfer of energy. It is thus anticipated that the rate of $^1\text{O}_2$ generation will be viscosity-dependent. Sulfur-containing compounds can also act as physical quenchers of $^1\text{O}_2$ through collisional inactivation.^{39,40} Thus, following the generation of $^1\text{O}_2$ by dithiaporphyrins, $^1\text{O}_2$ can diffuse away from the dithiaporphyrin and react with the DMA or can be physically quenched by dithiaporphyrin via collisional transfer of energy. As the porphyrin is buried deeper in the membrane, the effective viscosity increases, rates of diffusion decrease, and the percentage of $^1\text{O}_2$ to escape the local environment around the dithiaporphyrin decreases while the percentage quenched by the dithiaporphyrin increases.

To establish the validity of this hypothesis we measured the quantum yields for the generation of $^1\text{O}_2$ by **III** and **VI**, as representative cases, in liposomes, as a function of the photosensitizer's concentration (Table 3). Both photosensitizers showed a decrease in the quantum yield as their membrane-bound concentration increases. The decrease is more significant for **VI**, with the longer side chain. The quantum yield should be independent of concentration, unless the molecule is self-quenched by the photosensitizer and ensuing concentration dependence is to be observed, as is demonstrated in Table 3. This leads us to the conclusion that the photosensitizers, especially those with the longer side chains, are self-quenched. As a result, these dithiaporphyrins manifest lower efficiency of photosensitized oxidation of a membrane-bound singlet oxygen target, in spite of being located in a more favorable deep location in the membrane, as was determined by the FRET measurements.

Nevertheless, in all cases singlet oxygen is produced in liposomes, thus suggesting that all the photosensitizers could be candidates for PDT.

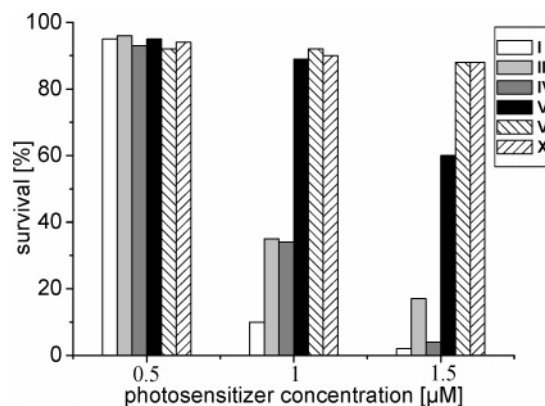


Figure 5. Dark toxicity test. The survival of U937 cells with various photosensitizer concentrations (0.5, 1, and 1.5 μM) after 24 h of incubation.

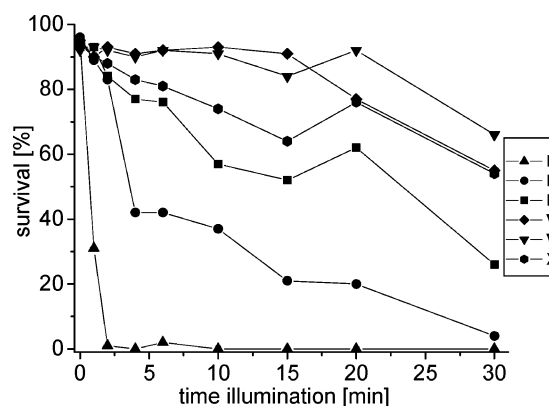


Figure 6. Phototoxicity test. U937 cells were incubated for 2 h with 0.5 μM photosensitizer and different illumination periods (0, 1, 2, 4, 6, 10, 15, 20, and 30 min) with 2.5 mW cm^{-2} of 380–480 nm light. After illumination we incubated the cells again for 20 h and then measured their viability. Error bars for 1 standard deviation are $<10\%$ and are omitted for clarity.

Dark Toxicity and Phototoxicity. The dithiaporphyrins of this study were evaluated for dark and phototoxicity toward U937 cells and R3230AC rat mammary adenocarcinoma cells. In order to minimize treatment times and to control heating of the cell samples, broad-band light (4.5 J cm^{-2} of 380–480 nm light for U937 cells and 3.8 J cm^{-2} of 350–750 nm light for R3230AC cells) was used with cell cultures rather than more narrow, band-4-specific beams. In actual applications of dithiaporphyrins for treatment in vivo, 135 J cm^{-2} of 694 nm light delivered at 75 mW cm^{-2} has been employed.¹³

U937 cells showed no dark toxicity upon incubation with 0.5 μM photosensitizer for 24 h. Incubation with higher concentrations of the photosensitizers for the same period of time showed dark toxicity, especially in sensitizers with shorter side chains (Figure 5).

Phototoxicity was measured following 2 h of incubation with 0.5 μM photosensitizer and different illumination periods (0, 1, 2, 4, 6, 10, 15, 20, and 30 min). After illumination we incubated the cells again for 20 h and then measured viability (Figure 6). **I** showed the highest phototoxicity and destroyed about 100% of the cells after illumination of only 2 min. **III** was the second most phototoxic photosensitizer with 95% of cells destroyed after 30 min of illumination. **IV** destroyed 74% of the cells after illumination for only 30 min. **V**, **VI**, and **X** were significantly less phototoxic and destroyed 45%, 33%, and 46% of the cells, respectively, after illumination of 30 min.

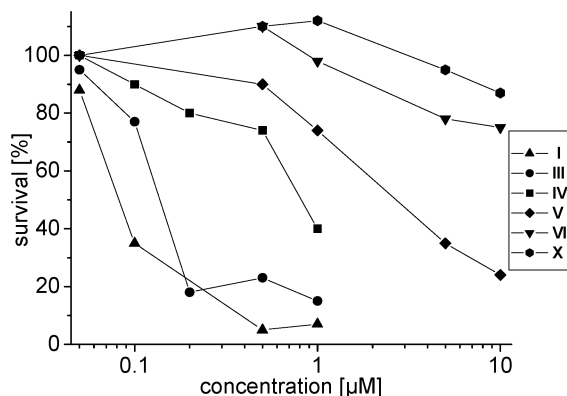


Figure 7. Phototoxicity test. R3230AC cells were incubated for 25 h with various concentrations of photosensitizer and illuminated with 3.8 J cm^{-2} of 350–750 nm light. After illumination cells were incubated for 24 h and then measured for viability. Error bars for 1 standard deviation are $<10\%$ and are omitted for clarity.

We also examined dark and phototoxicity in R3230AC rat mammary adenocarcinoma cells upon incubation with various concentrations of the photosensitizers. The R3230AC cells showed no dark toxicity upon incubation with 10 μM photosensitizer for 24 h. With the U937 cells, phototoxicity was measured as a function of light dose with constant photosensitizer concentration. With the R3230AC cells, phototoxicity was measured with a constant light dose (3.8 J cm^{-2} of filtered 350–750 nm light delivered at 1.4 mW cm^{-2}) and varying concentration of photosensitizer. Following illumination, cells were incubated for 24 h and then measured for viability. As with the U937 cells, **I** and **III** were the two most phototoxic compounds with 65% cell death with **I** at 0.1 μM and 80% cell death with **III** at 0.2 μM (Figure 7). Photosensitizer **IV** gave approximately 60% cell death at 1 μM , whereas **V** gave approximately 60% cell death at 5 μM . Photosensitizers **VI** and **X** displayed little phototoxicity at concentrations of 10 μM .

In both the U937 and R3230AC cells, a correlation exists between the side-chain length of the photosensitizer and the survival of the cells. The photosensitizers with shorter alkyl side chains (**I**, **III**, **IV**) are significantly more phototoxic than the photosensitizers with longer side chains (**X**, **VI**, **V**) as either a function of light dose (Figure 6) or photosensitizer concentration (Figure 7).

The uptake of the photosensitizers into the cell can be either by diffusion or by endocytosis. The higher phototoxicity of the shorter photosensitizers may be explained by their better diffusion into the cell membrane compared to photosensitizers with longer side chains and possibly also by more preferable subcellular localization. Due to the very weak fluorescence in cells, we could not determine the photosensitizers' subcellular localization by fluorescence microscopy. Since the binding of photosensitizers with longer side chains to liposomes is slow, we can assume that the uptake of the long sensitizers is done mainly by endocytosis. This difference affects the location of the photosensitizer in the cell and as a result the phototoxicity of the photosensitizer.

Conclusions

The elongation of the side chains that bind the carboxyl group to the phenol at positions 10 and 15 of the dithiaporphyrin has a small effect on the photophysical properties of the photosensitizers that are reported in this study. All photosensitizers (**I**, **III**, **IV**, **V**, **VI**, and **X**) have very similar absorption and emission spectra, and they possess almost the same quantum yields of

generation of $^1\text{O}_2$ in MeOH. However, the quantum yield of the generation of $^1\text{O}_2$ in liposomes was significantly affected by the structural differences between the photosensitizers. We observed a significant self-quenching of singlet oxygen when we measured the quantum yields of the generation of $^1\text{O}_2$ in liposomes. We found that the self-quenching depends on the side-chain length, which determines the depth of the photosensitizer's core in the bilayer. The longer the side chain, the deeper the photosensitizer's core is positioned in the bilayer and thus is more self-quenchable.

The photosensitizers with the shorter side chain, especially **I**, showed the highest photodynamic efficiency in two different cell lines. There are three possible reasons for the higher phototoxicity of the shorter photosensitizers: (1) Significant self-quenching of the photosensitizers with the longer side chain. (2) Better diffusion into the cell membrane of the photosensitizers with shorter side chains compared to the longer ones. (3) Different mechanisms by which the photosensitizers penetrate the cell, i.e., diffusion through the membrane or endocytosis. This affects the location of the photosensitizer in the cell and as a result the phototoxicity of the photosensitizer. Because of the unique property of these dithiaporphyrins to quench singlet oxygen, we obtain here the unusual situation that the deeper-seated sensitizers are not necessarily those that exhibit better membrane-bound photosensitized reaction. This is contrary to the trend that we have observed before in all cases, when sets of sensitizers with probable different locations in the membrane were studied.^{31–35}

Of all the photosensitizers of the series that was tested here, **I** seems to be the most promising sensitizer for PDT applications.

Acknowledgment. We thank Professor Mordechai Deutsch and Mrs. Pnina Lebovich from the Department of Physics at Bar Ilan University for supplying us with U937 cells and for using their biological hood. We would like to acknowledge the generous support (Grant No. 2002383) of the United States–Israel Binational Science Foundation (BSF), Jerusalem, Israel (to B.E.). We also acknowledge the support of the Michael David Falk Chair in Laser Phototherapy. This research was also supported in part by the Department of Defense (Breast Cancer Research Program) under Award No. W81XWH-04-1-0500 (to Y.Y.). Views and opinions of, and endorsements by, the author(s) do not reflect those of the U.S. Army or the Department of Defense.

References and Notes

- (1) Detty, M. R.; Gibson, S. L.; Wagner, S. J. *Med. Chem.* **2004**, *47*, 3897–3915.
- (2) Kato, H. J. *Photochem. Photobiol.*, **B** **1998**, *42*, 96–99.
- (3) Ost, D. *Methods Mol. Med.* **2003**, *75*, 507–526.
- (4) Probst, R. L.; Wolfson, H. C.; Gahlen, J. *Endoscopy* **2003**, *35*, 1059–1068.
- (5) Guillemin, F.; Feintrenie, X.; Lignon, D. *Rev. Pneumol. Clin.* **1992**, *48*, 111–114.
- (6) Henderson, B. W.; Dougherty, T. J. *Photochem. Photobiol.* **1992**, *55*, 145–157.
- (7) Dougherty, T. J.; Gomer, C. J.; Henderson, B. W.; Jori, G.; Kessel, D.; Korbek, M.; Moan, J.; Peng, Q. *J. Natl. Cancer Inst.* **1998**, *90*, 889–905.
- (8) Serman, W. M.; Allen, C. M.; van Lier, J. E. *Drug Discovery Today* **1999**, *4*, 507–517.
- (9) Stilts, C. E.; Nelen, M. I.; Hilmey, D. G.; Davies, S. R.; Gollnick, S. O.; Oseroff, A. R.; Gibson, S. L.; Hilf, R.; Detty, M. R. *J. Med. Chem.* **2000**, *43*, 2403–2410.
- (10) You, Y.; Gibson, S. L.; Hilf, R.; Davies, S. R.; Oseroff, A. R.; Roy, I.; Ohulchanskyy, T. Y.; Bergey, E. J.; Detty, M. R. *J. Med. Chem.* **2003**, *46*, 3734–3747.
- (11) You, Y.; Gibson, S. L.; Hilf, R.; Ohulchanskyy, T. Y.; Detty, M. R. *Bioorg. Med. Chem.* **2005**, *13*, 2235–2251.

- (12) Marcinkowska, E.; Ziolkowski, P.; Pacholska, E.; Latos-Grazynski, L.; Chmielewski, P.; Radzikowski, C. *Z. Anticancer Res.* **1997**, *17*, 3313–3320.
- (13) Hilmey, D. G.; Abe, M.; Nelen, M. I.; Stilts, C. E.; Baker, G. A.; Baker, S. N.; Bright, F. V.; Davies, S. R.; Gollnick, S. O.; Oseroff, A. R.; Gibson, S. L.; Hilf, R.; Detty, M. R. *J. Med. Chem.* **2002**, *45*, 449–461.
- (14) Ulman, A.; Manassen, J.; Frolow, F.; Rabinovich, D. *Tetrahedron Lett.* **1978**, *19*, 167–170.
- (15) Ulman, A.; Manassen, J.; Frolow, F.; Rabinovich, D. *Tetrahedron Lett.* **1978**, *19*, 1885–1886.
- (16) Wu, P.; Brand, L. *Anal. Biochem.* **1994**, *218*, 1–13.
- (17) Clegg, R. M. *Curr. Opin. Biotechnol.* **1995**, *6*, 103–110.
- (18) Clegg, R. M. Fluorescence Resonance Energy Transfer (FRET). In *Fluorescence Imaging Spectroscopy and Microscopy*; Wang, X. F., Herman, B., Eds.; Wiley: New York, 1996.
- (19) Kenworthy, A. K.; Edidin, M. *J. Cell Biol.* **1998**, *142*, 69–84.
- (20) Kenworthy, A. K.; Petranova, N.; Edidin, M. *Mol. Biol. Cell* **2000**, *11*, 1645–1655.
- (21) Wilkinson, F.; Helman, W. P.; Ross, A. B. *J. Phys. Chem. Ref. Data* **1995**, *24*, 663–1021.
- (22) Corey, E. J.; Taylor, W. T. *J. Am. Chem. Soc.* **1964**, *86*, 3881–3882.
- (23) Usui, Y. *Chem. Lett.* **1973**, 743–744.
- (24) Wilkinson, F.; Brummer, J. J. *Phys. Chem. Ref. Data* **1981**, *10*, 809–999.
- (25) Gross, E.; Ehrenberg, B.; Johnson, F. M. *Photochem. Photobiol.* **1993**, *57*, 808–813.
- (26) Wilkinson, F.; Brummer, J. J. *Phys. Chem. Ref. Data* **1981**, *22*, 113–262.
- (27) Bevington, P. R. *Data Reduction and Error Analysis for the Physical Sciences*; McGraw-Hill: New York, 1969; Chapter 5.
- (28) Mosmann, T. *J. Immunol. Methods* **1983**, *65*, 55–63.
- (29) Stein, W. D. *Transport and Diffusion across Cell Membranes*; Academic Press: New York, 1986.
- (30) Ehrenberg, B. *J. Photochem. Photobiol., B* **1992**, *14*, 383–386.
- (31) Lavi, A.; Weitman, H.; Holmes, R. T.; Smith, K. M.; Ehrenberg, B. *Biophys. J.* **2002**, *82*, 2101–2110.
- (32) Bronshtein, I.; Afri, M.; Weitman, H.; Frimer, A. A.; Smith, K. M.; Ehrenberg, B. *Biophys. J.* **2004**, *87*, 1155–1164.
- (33) Bronshtein, I.; Smith, K. M.; Ehrenberg, B. *Photochem. Photobiol.* **2005**, *81*, 446–451.
- (34) Bronshtein, I.; Aulova, S.; Juzeniene, A.; Iani, V.; Ma, L. W.; Smith, K. M.; Malik, Z.; Moan, J.; Ehrenberg, B. *Photochem. Photobiol.* **2006**, *82*, 1319–1325.
- (35) Sholto, A.; Lee, S.; Hoffman, B. M.; Barrett, A. G. M.; Ehrenberg, B. *Photochem. Photobiol.*, in press (DOI: 10.1111/j.1751-1097.2007.00268.x, 2008).
- (36) Pandey, R. K.; Sumlin, A. B.; Constantine, S.; Aoudia, M.; Potter, W. R.; Bellnier, D. A.; Henderson, B. W.; Rodgers, M. A.; Smith, K. M.; Dougherty, T. J. *Photochem. Photobiol.* **1996**, *64*, 194–204.
- (37) Dougherty, T. J. *Photochem. Photobiol.* **1987**, *45*, 879–889.
- (38) Vandenbogaerde, A. L.; Delaey, E. M.; Vantieghem, A. M.; Himpens, B. E.; Merlevede, W. J.; de Witte, P. A. *Photochem. Photobiol.* **1998**, *67*, 119–125.
- (39) Kacher, M. L.; Foote, C. S. *Photochem. Photobiol.* **1979**, *29*, 756–769.
- (40) Sergueievski, P.; Detty, M. R. *Organometallics* **1997**, *16*, 4386–4391.